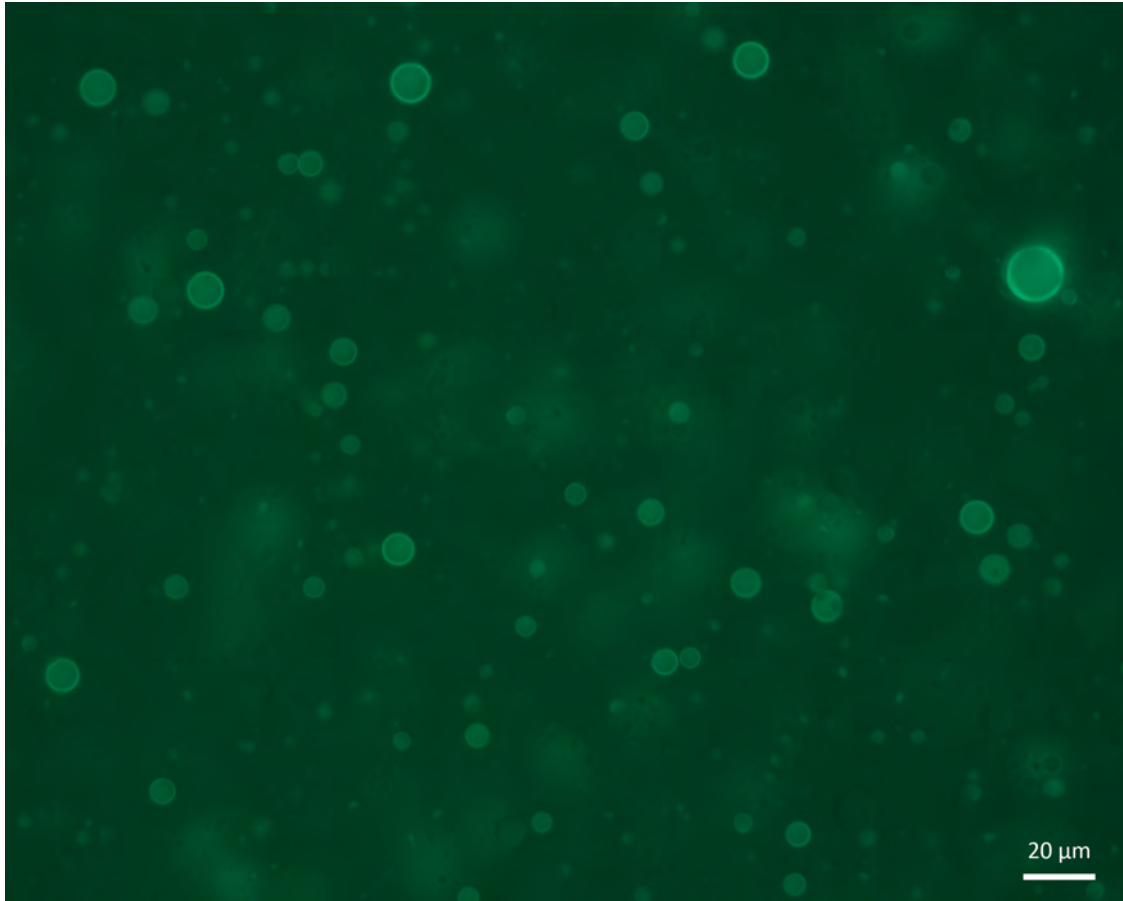




**CHALMERS**  
UNIVERSITY OF TECHNOLOGY

---



# UV-responsive Microcapsules

Methodology for formulation, characterization and triggered release investigation on a solid substrate

Master's thesis

ALINA BEER



MASTER'S THESIS 2017

## UV-responsive microcapsules

Methodology for formulation, characterization and triggered release  
investigation on a solid substrate

ALINA BEER



**CHALMERS**  
UNIVERSITY OF TECHNOLOGY

Department of Chemistry and Chemical Engineering  
*Division of Applied Surface Chemistry*  
CHALMERS UNIVERSITY OF TECHNOLOGY  
Gothenburg, Sweden 2017

UV-responsive microcapsules  
Methodology for formulation, characterization and triggered release investigation on  
a solid substrate  
ALINA BEER

© ALINA BEER, 2017.

Supervisors: Lars Nordstierna, Chalmers University of Technology  
Markus Andersson Trojer, Swerea IVF  
Examiner: Lars Nordstierna, Chalmers University of Technology

Master's Thesis 2017  
Department of Chemistry and Chemical Engineering  
Division of Applied Surface Chemistry  
Chalmers University of Technology  
SE-412 96 Gothenburg  
Telephone +46 31 772 1000

Cover: Fluorescence image of microcapsules with polyphthalaldehyde shells.

Gothenburg, Sweden 2017

## Abstract

Microcapsules that release their content on a solid surface once irradiated with UV light have potential applications in industry. Formation of UV-responsive microcapsules has been reported in literature, but it is very uncommon to trigger and investigate the release while they are in dry state. This thesis work have aimed to develop methodology to perform such experiments by producing microcapsules with shells from UV-responsive polymers and investigate their reaction to UV using optical microscopy. Poly(methyl methacrylate) (PMMA), polystyrene (PS) and polyphthalaldehyde (PPHA) was used as shell material to form microcapsules using internal phase separation by solvent evaporation technique. Production volume was scaled down to reduce polymer consumption. Different dyes and optical microscopy methods were evaluated to visualize the core oil. Methods for sample preparation and imaging the same spots before and after the trigger event were found. Finally, the reaction of produced microcapsules to UV was investigated. The most important findings are contained in remarks on using small volume setup, using optical microscopy for the release studies and formulation of PPHA microcapsules. The work provides a basis for further research in this topic.

Keywords: microcapsules, triggered release, UV, optical microscopy, internal phase separation, poly(methyl methacrylate), polystyrene, polyphthalaldehyde, Sudan I.



## Acknowledgements

First, I would like to thank my main supervisor and examiner Lars, who gave me a chance to work on this interesting project and helped me in a number of ways. Further, I would like to express my gratitude to Markus who also advised me and supported with optimism. I sincerely appreciate the guidance from both of you and I'm thankful that you would always find time for me.

I owe special thanks to Krzysztof for all the tips, discussions and unfailing support in the lab. I would also like to acknowledge Mats, Sanna, Romain and Gunnar - what I have learned from them was notably useful in this work.

I am very grateful to all the workers, PhD students and office colleagues from the Applied Chemistry division - it seems that everyone helped me in some way at some point or at least contributed to the good atmosphere. A very special thank you goes to Szilvia for being the best project mate I can imagine. I feel very lucky that I could meet all of you.

Finally, I would like to thank my friends and family who were there for me when I needed it. I am especially thankful to my dad for all the inspiring conversations and to my mom for the motivation, unconditional love and support.

Alina Beer, Gothenburg, October 2017





# Contents

<b>List of Figures</b>	<b>xi</b>
<b>List of Tables</b>	<b>xiii</b>
<b>1 Introduction</b>	<b>1</b>
<b>2 Background</b>	<b>3</b>
2.1 Microencapsulation . . . . .	3
2.1.1 Fabrication techniques . . . . .	3
2.1.2 Internal phase separation by solvent evaporation . . . . .	5
2.2 Colloidal stability . . . . .	7
2.2.1 Attractive forces . . . . .	7
2.2.2 Stabilization . . . . .	7
2.2.2.1 Electrostatic and steric stabilization . . . . .	7
2.2.2.2 Stabilization with particles . . . . .	9
2.2.3 Destabilization mechanisms . . . . .	10
2.3 Triggered release . . . . .	11
2.3.1 Strategies for triggered release . . . . .	11
2.3.2 UV responsive systems . . . . .	12
2.3.3 Photodegradation of polymers . . . . .	12
2.3.3.1 Photolysis . . . . .	12
2.3.3.2 Photooxidation . . . . .	13
2.3.3.3 Depolymerization . . . . .	14
2.4 Characterization techniques . . . . .	15
2.4.1 Optical microscopy . . . . .	15
2.4.1.1 Instrument components . . . . .	15
2.4.1.2 Fluorescence and fluorophores . . . . .	16
2.4.2 Dynamic light scattering (DLS) . . . . .	16
<b>3 Methods</b>	<b>17</b>
3.1 Preparation of microcapsules . . . . .	17
3.1.1 Materials . . . . .	17
3.1.2 Procedure . . . . .	17
3.1.3 Comments regarding working on small volumes . . . . .	18
3.1.4 Experiments with TiO <sub>2</sub> nanoparticles as emulsifier . . . . .	19
3.2 Characterization with optical microscopy . . . . .	20
3.2.1 Equipment . . . . .	20

3.2.2	Methods . . . . .	20
3.3	Release studies . . . . .	21
3.3.1	Preparation of dry microcapsules monolayer . . . . .	21
3.3.2	Triggered release investigation . . . . .	21
<b>4</b>	<b>Results and discussion</b>	<b>23</b>
4.1	Formulation of reference microcapsules with PMMA shells . . . . .	23
4.1.1	Dyes . . . . .	23
4.1.2	Core materials . . . . .	27
4.1.3	Dispersants . . . . .	28
4.1.4	Rotation speed and emulsification time . . . . .	29
4.1.5	Optimization of production in small volume setup . . . . .	30
4.2	Formulation of microcapsules with UV sensitive components . . . . .	32
4.2.1	PS shells, thinner shell walls and TiO <sub>2</sub> as emulsifier . . . . .	32
4.2.1.1	Microcapsules with PS shells . . . . .	32
4.2.1.2	Pickering emulsion with TiO <sub>2</sub> . . . . .	33
4.2.2	Microcapsules with PPHA shells . . . . .	34
4.3	Using optical microscopy for characterization and visualization of re- leased core materials . . . . .	35
4.4	Methodology for studying the release from dry microcapsules . . . . .	36
4.5	Response of microcapsules and their components to UV . . . . .	38
4.5.1	Sudan I . . . . .	38
4.5.2	PMMA microcapsules . . . . .	39
4.5.3	PS microcapsules . . . . .	41
4.5.4	PPHA microcapsules . . . . .	42
<b>5</b>	<b>Conclusion</b>	<b>43</b>
	<b>Bibliography</b>	<b>45</b>
	<b>Appendix A: Formulation details</b>	<b>I</b>

# List of Figures

2.1	Basic internal morphologies of microcapsules: A1 - matrix/monolithic (microsphere); A2 - core-shell; A3 - multicore; A4 - core-multishell [9].	3
2.2	The process of shell formation in solvent evaporation technique [18].	5
2.3	Different outcomes of encapsulation: core-shell particle, acorn particle and phase separation [19].	6
2.4	Simplified mechanism of osmotic barrier stabilization in electrostatic (a) and steric (b) system [22].	8
2.5	Scheme of a droplet stabilized with solid particles (a) and the relation between contact angle $\theta$ and position of the particle in the colloidal system [22].	9
2.6	Scission of PMMA backbone [41].	13
2.7	Typical steps of photooxidation degradation [42].	13
2.8	Scheme of PPHA depolymerization induced by removal of the end-cap (trigger) group [51].	14
2.9	Components of a typical optical microscope operating in transmission mode (left) and a microscope with equipment necessary for capturing fluorescence images operating in reflectance mode (right) [52].	15
4.1	Bright field (left) and fluorescence (right) images of microcapsules with Disperse Red 13 added in small amount (a,b) and in large amount (c,d).	24
4.2	Bright field and fluorescence images of microcapsules with $\beta$ -carotene.	24
4.3	Bright field and fluorescence images of microcapsules with Sudan I.	25
4.4	Particles from the batch with large amount of Disperse Red added to the oil phase - region of suspension where acorn-like particles were present.	26
4.5	Microcapsules with possibly higher ( $>3.3$ g/l of HD) concentration of Sudan I (a) and with impurities in the emulsion (b). The scale bar is 50 $\mu$ m.	27
4.6	Microcapsules with HD cores with visible indentations (a) and microcapsules with OMCTS cores (b).	27
4.7	DIC images of emulsion stabilized with PMAA (a) and PVA (b) captured shortly ( $<15$ min) after homogenization.	28
4.8	DIC images of microcapsules stabilized with PMAA (a) and PVA (b).	28
4.9	Emulsions sampled after 2min (a), 10min (b) and 60min (c) of homogenization.	29

4.10	Emulsion produced in small volume setup after 60min (a) and 90min (b) of homogenization. The big spheres that are not yellow can be air bubbles. . . . .	30
4.11	Suspension of microcapsules with Sudan I obtained at an early stage of small volume setup tests (a) and after optimization of the production method. The scale bar is 200 $\mu\text{m}$ . . . . .	31
4.12	PS microcapsules with Sudan I with standard shell thickness (a) and with thinner shells (b). . . . .	32
4.13	Effect of attempt to form Pickering emulsion with $\text{TiO}_2$ nanoparticles. . . . .	33
4.14	Fluorescence images of microcapsules with PPHA shells: standard recipe (a), batch where DCM was rotary evaporated (b), batch with higher polymer-core oil ratio (c), batch with lycopene (d). The scale bar is 20 $\mu\text{m}$ . . . . .	34
4.15	PMMA microcapsules with Sudan I before (a) and after (b) adding a drop of methanol. . . . .	37
4.16	Image of the boundary between mechanically crushed (bottom) and unaffected (top) region of PS microcapsules with Sudan I, obtained by superimposing bright field and fluorescence image. . . . .	37
4.17	Increase of fluorescence intensity of PS microcapsules with Sudan I before UV (left) and consecutively: after 10 min, 30 min and 60 min of UV irradiation. . . . .	38
4.18	Sudan I dissolved in HD before (a) and after (b) 1.5h of UV irradiation. . . . .	39
4.19	Bright field image of PMMA microcapsules (diameter 10 $\mu\text{m}$ ) before (a) and after (b) 5h of UV irradiation. . . . .	39
4.20	PMMA microcapsules stabilized with PVA, before (a) and after (b) 5h of UV irradiation. . . . .	39
4.21	PMMA microcapsules stabilized with PMAA, before (a, c, e) and after (b, d, f) 5h of UV irradiation (particle diameters: 5-10 $\mu\text{m}$ ). . . . .	40
4.22	Bright field image of a PS microcapsule (diameter 10 $\mu\text{m}$ ) before (a) and after (b) 4h of UV irradiation. . . . .	41
4.23	Thin-shell PS microcapsules before (a) and after (b) 4h of UV irradiation. . . . .	41
4.24	PPHA microcapsules without dye before (a) and after (b) 1.5h of UV irradiation. . . . .	42

# List of Tables

.1	Composition and parameters used to produce microcapsules . . . . .	I
.2	Typical emulsion composition ( $M_S/M_C = 0.66$ ) for large- and small volume setup . . . . .	II



# 1

## Introduction

Microcapsules that release a liquid content in response to some specific stimuli are of significant interest for various industrial applications such as self-healing materials, drug delivery, agriculture, deodorants, cosmetics and delivery of anti-corrosive materials [1]. Microcapsules can be designed to respond to stimuli such as light, chemicals, temperature, magnetic or electric field. UV light allows to trigger the release remotely, without heat generation, what gives it an advantage over other approaches in those applications where rise in temperature is unfavorable.

Formation of UV-sensitive microcapsules have been reported in literature [2]–[5], but most groups studied the release from capsules suspended in a liquid, and based their results on measurements of increased permeation of an active substance to the medium, or on potentially shell-damaging electron microscopy observations. Those methods are not optimal if in the intended application the release occurs from dry microcapsules on a solid surface, and when it is important that the released material forms a uniform layer. More suitable here would be a direct observation under optical microscopy, but this approach is very uncommon in triggered release studies - the only example found by the author is in a work of Pastine *et al.* [6], where burst release was observed under optical microscope during irradiation with near-IR laser.

The aim of this thesis is to develop a methodology to use UV-responsive polymers to produce microcapsules, to test their reaction to UV irradiation, and to investigate triggered release from the dry capsules using optical microscopy. Initial experiments, performed on common PMMA as shell material, are focused on choosing appropriate dye, tuning the capsule size and scaling down the production volume to reduce polymer consumption. Next, microcapsules from polymers that are more sensitive to UV (PS and PPHA [7]) are produced. An attempt to incorporate photocatalytic TiO<sub>2</sub> nanoparticles on shell surface is also performed. The work suggests an easy method for sample preparation and explores the optimal way to use optical microscope for the purpose of released core visualization. The thesis does not engage with quantitative measurements of released actives. The results of preliminary irradiation experiments are presented in form of images of the same particles before and after application of a stimuli.

The next chapter contains background information and introduces relevant theoretical concepts. It is followed by a detailed description of methodology in Chapter 3. The results are presented and discussed in Chapter 4. Finally, the main findings and suggestions for future work are gathered in the Conclusion chapter.





# 2

## Background

### 2.1 Microencapsulation

Microencapsulation is a method of isolating a gaseous, liquid or solid material from its surroundings by packaging it into capsules of another one. The protective shell is typically polymeric, but inorganic and composite materials are also used. Microcapsules may have spherical or irregular shape and their size is in a range of 1-1000  $\mu\text{m}$ . Capsules bigger than that are classified as macrocapsules or beads, while smaller are called nanocapsules [8].

Microcapsules may have different internal morphologies, which can be achieved by adjusting composition and manufacturing parameters. The basic structures are presented on Fig.2.1. Microspheres, multicore and multishell morphologies can be desirable when the purpose is to slow down the release of an active. In this project, the aim is to obtain microcapsules that would release a liquid core instantaneously after UV irradiation, so only core-shell particles are taken under consideration.

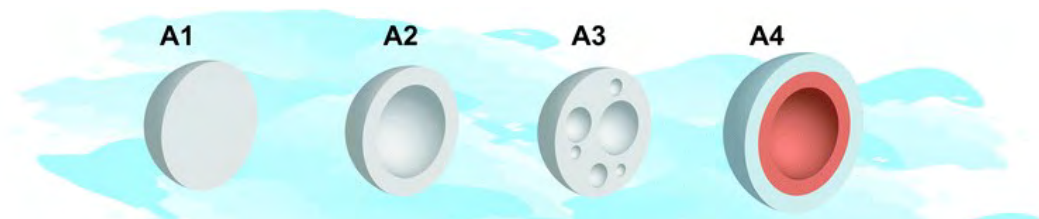


**Figure 2.1:** Basic internal morphologies of microcapsules: A1 - matrix/monolithic (microsphere); A2 - core-shell; A3 - multicore; A4 - core-multishell [9].

#### 2.1.1 Fabrication techniques

While choosing the encapsulation technique, factors such as desired morphology, specificity of component materials or production scale must be considered. Numerous methods for production of microcapsules are reported in literature [8]. Some reviews focus exclusively on techniques used to produce core-shell particles [10], [11]. In this subsection the main approaches to produce microcapsules with polymeric shells and liquid cores are introduced. Some techniques are omitted, because they are more suitable to obtain matrix-type and polynuclear morphologies (e.g. spraying [8]), limit the polymer choice to water-soluble ones (coacervation [12]), or are used to obtain capsules with radius bigger than 50  $\mu\text{m}$  (microfluidics [13]).

### *Internal phase separation*

There are few variations of this approach [11], but the basic principle is the same - core-shell structure is achieved due to separation of the polymer phase inside an emulsion droplet and its migration to the oil/water interface. The phase separation is usually induced by polymerization or solvent removal. In the former method, the emulsion droplets contain dissolved monomer, which after reaction initiation transform into an insoluble polymer. The latter technique requires dissolution of the shell and oil material in a good solvent, which is extracted or evaporated after emulsification. An alternative is to use photo-responsive polymers that alter their solubility through trans-to-cis isomerization [14]. Most of these systems are based on oil-in-water emulsions resulting in microcapsules with oil core, but it is possible to obtain aqueous cores using a double emulsion technique [15].

### *Interfacial polymerization in emulsions*

Shell is formed at the emulsion droplet interface due to condensation reaction between water-soluble and oil-soluble reactants. Once a polymeric film is created around the droplet, the reactants cannot meet readily and polymerization rate decreases. Because of that, final shell thickness and particle size can be easily controlled. Limitation of this method arise from the fact that the microcapsules may contain remains of unreacted monomer [16].

### *Layer-by-layer deposition (LbL)*

In this technique the encapsulation is achieved by deposition of polyelectrolyte layers onto emulsion droplets. Alternating layers of oppositely charged molecules can be employed to create robust shells of required thickness and porosity. Unadsorbed polyelectrolytes have to be removed before next layer is added, what usually involves time consuming centrifugation and washing or microfiltration after each step. It is pointed out in literature that the production rate can be further affected by tendency of the particles to flocculate, resulting in necessity to work on low capsule concentrations [11].

### *Colloidosomes*

First an emulsion is formed, where aqueous phase contains dispersed polymer particles. After addition of the organic phase, the particles migrate to newly created interface and stabilize emulsion droplets. In next step the particles are fused, e.g. by heating the mixture above polymer glass transition temperature. Obtained shells will contain "holes", the size of which can be controlled by process parameters [17].

In this work all encapsulation batches were prepared with internal phase separation by solvent evaporation technique, since it is very versatile and does not require polymerization or heating step. Those characteristics are convenient when uncommon, stimuli-sensitive polymers are used.

### 2.1.2 Internal phase separation by solvent evaporation

The internal phase separation by solvent evaporation method was systematically studied and developed by Loxley and Vincent [12]. The basis of this technique is presented on Fig.2.2. The oil phase of an o/w emulsion consists of a polymer (shell material), volatile good solvent for the polymer and non-volatile poor solvent for the polymer (core material). Sufficient amount of good solvent is necessary to have the polymer completely dissolved. The water phase contains a dispersant to stabilize the emulsion droplets. After emulsification, the evaporation of volatile solvent through the aqueous phase leads to separation of polymer-rich phase inside the droplets and its migration towards the interface. Once the high vapor pressure solvent is completely removed, a core-shell microcapsule is obtained.

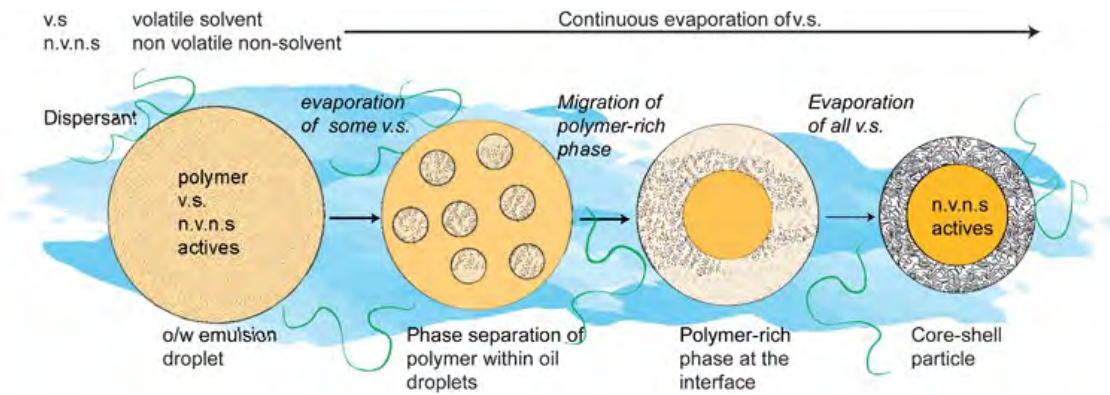


**Figure 2.2:** The process of shell formation in solvent evaporation technique [18].

The key to successful encapsulation is to provide conditions in which polymer ( $p$ ) spreads uniformly between the oil core ( $o$ ) and water phase ( $w$ ). Relative magnitudes of three interfacial tensions play a role here:  $\gamma_{ow}$ ,  $\gamma_{po}$  and  $\gamma_{pw}$ . To avoid formation of oil-water interface,  $\gamma_{ow}$  must be higher than  $\gamma_{po}$  and  $\gamma_{pw}$ . This can be expressed in terms of spreading coefficients as presented below:

The spreading coefficient for the polymer is defined as:

$$S_p = \gamma_{ow} - (\gamma_{po} + \gamma_{pw}) \quad (2.1)$$

Coefficients  $S_o$  and  $S_w$  are derived analogously. When we assume that  $\gamma_{ow} > \gamma_{pw}$  three combinations are possible:

$$S_o < 0 \quad S_w < 0 \quad S_p > 0 \quad (2.2)$$

$$S_o < 0 \quad S_w < 0 \quad S_p < 0 \quad (2.3)$$

$$S_o < 0 \quad S_w > 0 \quad S_p < 0 \quad (2.4)$$

## 2. Background

---

Core shell particles are formed when conditions in Equation 2.2 are satisfied. Conditions corresponding to Equation 2.3 result in, so called, acorn particles, while those from Equation 2.4 give separate polymer and oil droplets [12]. The three outcomes are presented on Figure 2.3.

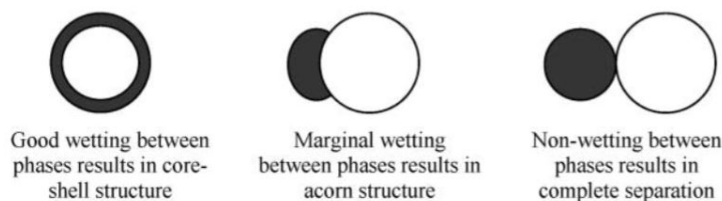


**Figure 2.3:** Different outcomes of encapsulation: core-shell particle, acorn particle and phase separation [19].

The importance of interfacial tensions in obtaining desired product imposes limitations on choice of the emulsifier. Traditional surfactants would lower  $\gamma_{ow}$  too much, hence water-soluble polymers such as polyvinyl alcohol or poly(methacrylic acid) are often employed to stabilize the emulsion. Moreover, it was reported that  $\gamma_{ow}$  can be lowered by impurities in starting materials [20], so in some cases their removal prior to use is practiced [12].

Properties of microcapsules prepared by solvent evaporation method can be controlled with composition and process parameters. For example, required shell thickness can be achieved by adjustment of core-to-shell ratio, while porosity will depend on solvent evaporation rate and on molecular weight (Mw) of used polymer. Factors affecting size of the microcapsules, such as reactor design, stirrer speed, additives, polymer Mw and content, or dispersant type and concentration are also described in literature [12], [21].

## 2.2 Colloidal stability

Stability of colloids plays an important role in emulsion formation, prevention of microcapsule aggregation and in dispersion of nanoparticles in water. Therefore, relevant theoretical concepts from this field are introduced in this section.

### 2.2.1 Attractive forces

In colloidal systems, electrostatic forces and Van der Waals forces play an important role. The force that is always present is London dispersion force, which arises from the fact that electrons are constantly moving in a molecule, creating a temporary dipole which induces dipoles in neighbouring molecules. Attraction force between particles is a sum of those different forces integrated over all their space. For two particles the attraction can be expressed by following equation:

$$U = \frac{A_H}{6h} \frac{R_1 R_2}{(R_1 + R_2)} \quad (2.5)$$

Here  $h$  stands for the distance between particles,  $R_1$  and  $R_2$  are their sizes, and  $A_H$  is the Hamaker constant defined as:

$$A_H = C \rho_1 \rho_2 \quad (2.6)$$

where  $C$  is the integral over different Van der Waals interactions, and  $\rho_1$  and  $\rho_2$  are atomic densities of the particles. It can be noticed that the attraction between particles is increasing with their size and decreasing as the distance between them is increased. Last but not least, the Hamaker constant of given material plays an important role in the magnitude of the attraction force.

It is worth noting that when particles approach each other in a medium, they have to replace solvent molecules, and so, Hamaker constant of given material will be smaller. Nevertheless, it will be always positive [22]. Because there is no repulsion between uncharged particles of the same material submerged in a medium, they have to be stabilized in order to obtain a stable suspension (for solid particles) or emulsion (for liquid droplets).

## 2.2.2 Stabilization

### 2.2.2.1 Electrostatic and steric stabilization

Two mechanisms of stabilization can be distinguished: electrostatic stabilization and steric stabilization. The two routes can be combined and then a term electrosteric stabilization is used. Both approaches are based on formation of an osmotic barrier, meaning that the flow of water seeking to dilute the region between particles is the actual stabilizing factor [22]. This is schematically illustrated on Figure 2.4 for both stabilization systems.

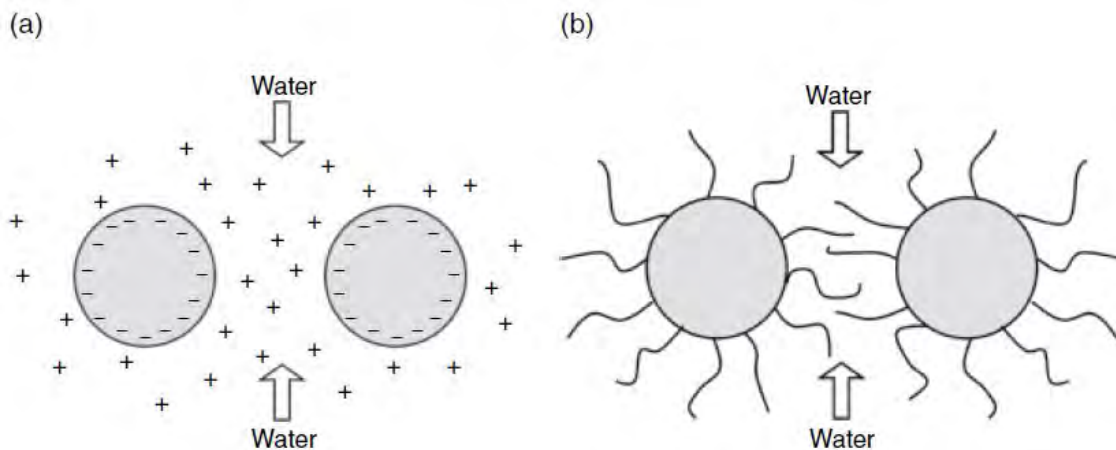


**Figure 2.4:** Simplified mechanism of osmotic barrier stabilization in electrostatic (a) and steric (b) system [22].

In electrostatic route the osmotic pressure is created because charged colloid particles are surrounded by "cloud" of counterions, often referred to as diffused part of electrical double layer (EDL) in literature. When the particles get closer to each other these layers overlap resulting in high local concentration of ions that water will seek to dilute. The thickness of EDL is decreasing with increasing electrolyte concentration, and presence of electrolytes can lead to destabilization of colloids in this system [23]. There are several means by which one can modify charge on material surface, changing the pH of suspending medium being one of them [24]. The net interaction resulting from combination of attractive Van der Waals forces with repulsive forces of EDL is quantitatively described in DLVO theory (named after Derjaguin, Landau, Verwey and Overbeek who worked on it). According to DLVO, for suspension in low ionic strength medium, repulsive forces dominate at large and intermediate distances, while attractive forces dominate at small distances. When ionic strength of a medium is high a weak attraction can appear at large distances, while behaviour at intermediate and small differences remains the same as in case of electrolyte-free system [22].

In case of steric stabilization, polymers are adsorbed on particle surface, and it is the high concentration of their segments that creates the osmotic pressure when particles get close to each other. There are another contributions to stabilization effect in steric systems apart from the osmotic mechanism. Reduction of conformational freedom of adsorbed polymers when particles are close to each other is one of them, however it is not clear if it is significant in practice. Another contribution may come from the positive free energy of desorption of the stabilizer that can occur when particles collide [25]. While electrostatically stabilized colloids were sensitive to electrolyte concentration, the stability of steric systems can be affected by temperature. It has been proven that at theta temperature (temperature at which polymer coil act like ideal chain and free energy change is equal to zero) sterically stabilized colloids undergo reversible flocculation [22], [25].

### 2.2.2.2 Stabilization with particles

An alternative approach to stabilize liquid droplets is based on reduction of O/W interface by adsorption of solid particles. Such system is commonly called a Pickering emulsion after S.U. Pickering who described the phenomena in 1907 [26]. The exact mechanism of the stabilization effect is still an area of research. It has been attributed to reduction of O/W interfacial tension [27], [28], increase in viscosity resulting in a kinetic barrier [29], [30], and to particle adsorption mechanism itself. Coalescence of emulsion droplets in Pickering emulsions is hindered by energy necessary to desorb particles from the O/W interface. The stabilization energy is expressed by following formula:

$$\Delta E = \pi r^2 \gamma (1 - |\cos\theta|)^2 \quad (2.7)$$

where  $r$  is the radius of stabilizing particles,  $\gamma$  represents the interfacial tension, and  $\theta$  is the contact angle between the interface and particle surface (see Figure 2.5). It can be noticed that large particle radius, large interfacial tension and  $90^\circ$  contact angle are beneficial for stability of the system. In practice, too big particles will not reach the interface in sufficient time, and unmodified interfacial tension may not allow to obtain small droplets. A common approximation is that the diameter of the particles should be 10 - 100 times smaller than diameter of the emulsion droplets, and additional emulsifiers are often used to reduce the interfacial tension [22].

In all cases it is important to make sure that the particle is wetted both by oil phase and water phase ( $\theta$  close to  $90^\circ$ ), keeping in mind that the more poorly wetting liquid should be the dispersed phase [31]. It is also worth noting that it has been reported that best stabilization effects are achieved when particles are in a state of incipient flocculation [32].

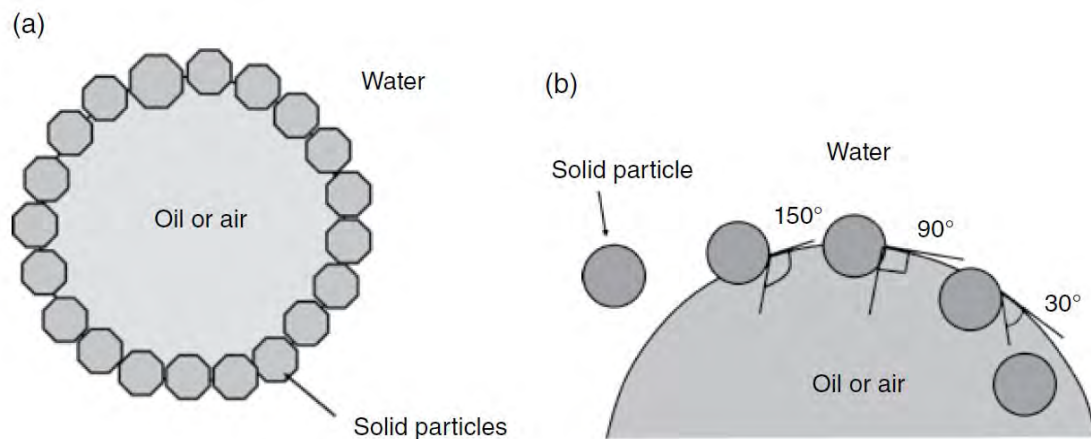


**Figure 2.5:** Scheme of a droplet stabilized with solid particles (a) and the relation between contact angle  $\theta$  and position of the particle in the colloidal system [22]

### 2.2.3 Destabilization mechanisms

Colloidal dispersions can be destabilized by several mechanisms [22]. For solid particles (microcapsules and  $\text{TiO}_2$  nanoparticles) it is important to distinguish between coagulation and flocculation. The former one is when stabilization is not sufficient and particles form condensed, difficult to break agglomerates. The latter one is when particles are attached to each other but certain distance is preserved, so that more "loose" networks are formed that can be redispersed.

Flocculation is common for systems stabilized with polymers. As noted in 2.2.2.1, it can occur when theta conditions are preserved. Other mechanisms are termed as bridging-, patch- and depletion flocculation. Bridging flocculation occurs when polymer adsorbs to two particles, what can happen when its molecular weight exceeds  $10^6$ . Patch flocculation is relevant for polyelectrolytes - when only parts of particles are covered with the stabilizer, oppositely charged patches will attract each other. The last mechanism, depletion, is related with excess of nonadsorbed polymer in the continuous phase. When two particles get close to each other and there is no polymer molecule between them, water will flow outside this region to dilute the polymer-rich surrounding, causing the particles approach even closer.

Sedimentation and creaming are destabilization mechanisms that can be observed in emulsions, microcapsule suspensions and  $\text{TiO}_2$  dispersions. If dispersed phase is more dense than liquid it will sediment, while in the opposite case creaming occurs. At last, coalescence is a mechanism typical for emulsion systems - it happens when droplets of the dispersed phase merge together to create bigger ones.



## 2.3 Triggered release

Release of microcapsule core "on-demand" can be achieved by implementing different strategies or their combinations. The main assumption of this project was to use UV light as a stimuli, with a focus on systems employing photosensitive polymer shells. Therefore, this section contains only brief summary of other approaches to triggered release, followed by short introduction of photodegradation mechanisms of polymers used in this work.

### 2.3.1 Strategies for triggered release

Various approaches to make capsules that release their content when a stimuli is applied have been reviewed by Esser-Kahn *et al.*[1]. They can be roughly categorized into two groups: those based on chemical reactions in the shell and those based on macroscopic physical changes of microcapsule components.

The chemical change route often involves depolymerization, cleavage of cross-links or so called switching reactions. Depolymerization mechanism is possible to use in case of low ceiling temperature polymers with protective end groups, and it is described in Section 2.3.3.3. Shell disintegration through removal of crosslinks can be achieved by reduction of disulfide bonds [33], acid mediated cleavage of acetals [34], base mediated hydrolysis of carbonate esters [35], or light induced cleavage of cinnamates [2]. The idea behind the last approach, switching, is to employ reactions that lead to reversible structural changes in the shell. Light induced cis-trans isomerization of an azo dye leading to porosity alteration is an example of such approach [36].

The group of macroscopic physical changes includes approaches such as mechanical cracking due to physical damage or melting of the shell, which are very straightforward and do not require explanation. The other ones can be termed as internal pressure induced rupture, change in porosity due to shrinkage, and thermomechanical degradation. Pressure induced burst of a capsules is usually triggered thermally and can occur due to vaporization of the liquid core or by contraction of the shell material. The porosity alteration due to shrinkage is usually achieved in systems where shell is made of two polymers mixture or a diblock polymer, where the components differ in their reaction to heating. At last, the term thermomechanical degradation is used for systems where nanoparticles are incorporated in the shell material, and their oscillations induced by magnetic or electric field lead to its heating and tearing [1].

The release mechanisms described above can be triggered by chemicals, biomolecules, changes in temperature, light, ultrasounds, and magnetic or electric field. In practice, it can be important that some of the stimuli involve direct interaction with the capsules (e.g. applying shear force) or alteration of the medium in which they are suspended (e.g. change in pH or presence of specific enzymes), while other act remotely (magnetic or electromagnetic field) [37].

### 2.3.2 UV responsive systems

The effect of UV irradiation on a polymer depends on wavelength and intensity of the UV light, as well as on structure of the molecule. It is possible to cleave saturated bonds in a process called laser ablation, where intense light of wavelength below 200 nm (far-UV) is used. However, this process is destructive to all organic molecules around, and hence not suitable for applications involving microencapsulation. Longer, less energetic near-UV (>200 nm) lasers can be used for purposes of triggered release, but it has to be done cautiously. It was pointed out in literature, that using a pulsed laser operating at 355 nm and energy density sufficient to affect shell wall can damage encapsulated substance as well [37]. For that reason, continuous wave lasers and lamps operating in near-UV region are the preferred radiation sources. Nonetheless, the milder approaches impose the need to use specially designed polymers or additives to attain shell degradation.

Depolymerizable polymers [38] and polymers containing UV absorbing chromophore units [3] have been shown to be promising UV reactive systems. There is also some research showing that incorporation of azobenzene moieties in the polymer shell provides a way of controlling microcapsule permeability with visible light and near-UV [36], [37]. Another route is addition of titanium dioxide nanoparticles to the system [39], which is known for its catalytic activity and strong oxidative potential upon UV irradiation due to electron-hole pair formation. An alternative is to use silver nanoparticles, since they absorb light in the range of near-UV and produce heat that affects the wall. Similar mechanism applies to gold nanoparticles, but their absorption is predominantly in the visible region [37]. Detailed overview of advances in using light of different wavelengths to trigger release from microcapsules can be found in reviews by Esser-Kahn *et al.* [1] and Bédard *et al.* [37]. A review focused on UV-responsive LbL capsules has been written by Yi and Sukhorukov [5].

### 2.3.3 Photodegradation of polymers

Photolysis, photooxidation and depolymerization are the main mechanisms behind degradation of shell materials used in this project. In this subsection they are shortly introduced.

#### 2.3.3.1 Photolysis

Photolysis is when a molecule is broken down directly by incident photons. It is the main photodegradation mechanism for PMMA used in this work [7]. In case of this polymer, scission can occur in the main chain (see Figure 2.6), or in methyl and ester side chains. Scission of a polymer backbone can be followed by depolymerization, however for commodity polymers the unzipping is of short-range (according to some studies max. 5 monomers per scission for PMMA)[40].

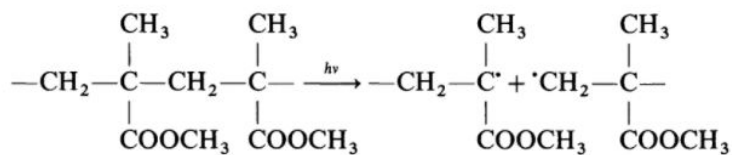


**Figure 2.6:** Scission of PMMA backbone [41].

### 2.3.3.2 Photooxidation

Most polymers undergo photooxidative degradation when exposed to UV in presence of air. It is often associated with chain scission, secondary oxidative reactions and formation of crosslinks. The simplified version of possible photooxidation reaction steps is presented on Figure 2.7. The initiation occurs when photons are absorbed by a chromophoric group and free radicals are formed. Reaction propagates as the free radical reacts with oxygen to generate polymer peroxy radical (POO●) that further react with polymer molecule to form a hydroperoxide (POOH) and a new polymer radical. POOH undergoes photolysis to produce polymer oxy radical (PO●) and hydroxy radical (HO●), what can result in chain branching. The degradation reaction is terminated when radicals react with each other - at this step crosslinks can be formed. Typically carbonyl groups can be detected in photooxidated polymers [42], [43].

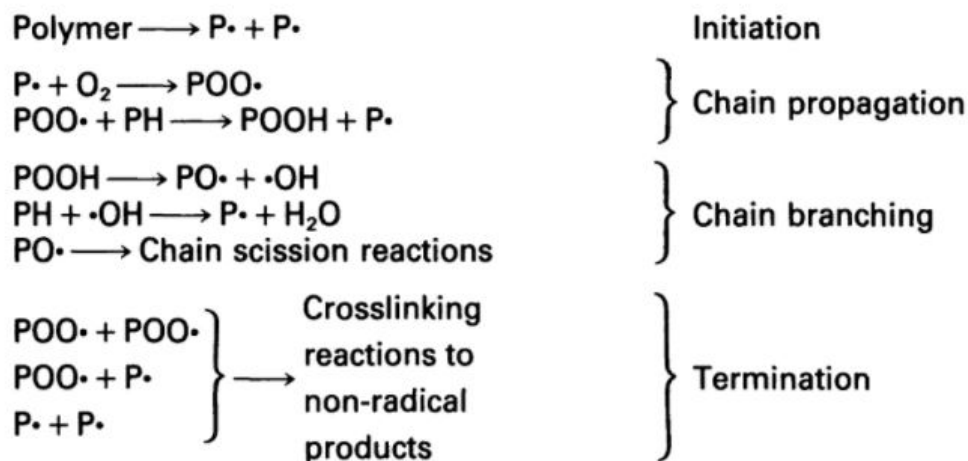


**Figure 2.7:** Typical steps of photooxidation degradation [42].

Detailed descriptions of PMMA [44] and PS [43] photooxidation can be found in literature. However, it was concluded in a study of materials used in this project, that from those two only PS undergoes photooxidative degradation after UV irradiation with HBO lamp [7]. It is worth noting that photooxidation can be hindered by presence of UV absorbing molecules, such as dyes and pigments. Antioxidants can also stabilize the polymers against degradation by reacting with radicals and forming inactive products [43].

### 2.3.3.3 Depolymerization

Depolymerization is a thermodynamic process in which polymer is converted into monomers. It occurs above ceiling temperature ( $T_c$ ) of given polymer, that is at temperature at which enthalpy of polymerization is outmatched by the entropy term ( $T\Delta S$ ) associated with conversion of macromolecule into monomers. For most polymers  $T_c$  is very high (e.g. 310°C for styrene) [45], but there is a special class of polymers, called depolymerizable or low ceiling temperature polymers, that have  $T_c$  close to- or below room temperature. Their chains have protective end groups (caps), so that depolymerization does not occur until their removal.

Depolymerizable polymers are closely related to self-immolative polymers. They both unzip into small molecules after end caps are removed, but in case of the former one parent monomers are obtained, while in the latter one other molecules can be produced [46], such as  $\text{CO}_2$ . The release of gaseous products is often the driving force for further unzipping in self-immolative polymers [47]. However, it happens in literature that terms *depolymerizable* and *self-immolative* are used interchangeably.

Polyphthalaldehyde, used in this project, has very low  $T_c$  (even -40°C according to some sources [48]). Once the protective group is removed at room temperature, it undergoes spontaneous head-to-tail depolymerization, which can be attributed to instability of the hemiacetal termini (see Figure 2.8). There are two routes to initiate PPHA depolymerization: chain scission or removal of stimuli-responsive end-cap. Chain scission can be achieved by mechanical means (e.g. through ultrasonication [49]) or by exposing the polymer to acid [50]. The second approach opens up the possibility to use various stimuli, provided that appropriate groups (triggers) are used for end-capping [48].

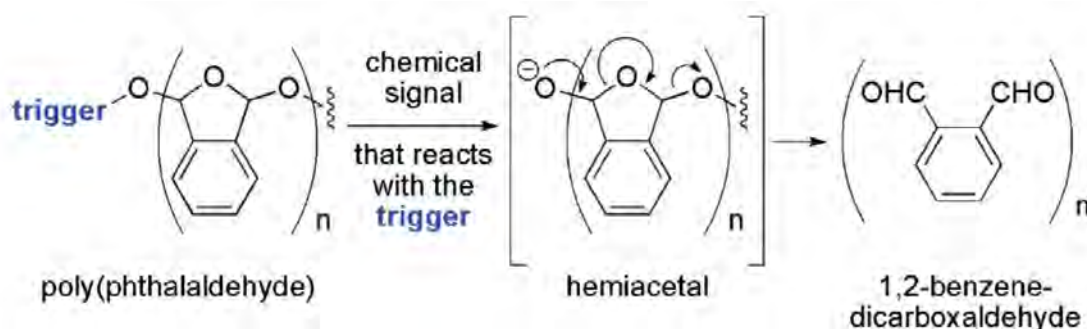


**Figure 2.8:** Scheme of PPHA depolymerization induced by removal of the end-cap (trigger) group [51].

## 2.4 Characterization techniques

This section introduces characterization techniques used in the thesis. The main one was optical microscopy, used for characterization of emulsions, microcapsule suspensions and for investigation of reaction of dry capsules to UV. Fluorescence mode was often used, hence short subsection about this technique and fluorophores is included. Dynamic light scattering (DLS) was only used to check if dispersion  $\text{TiO}_2$  nanoparticles was successful, so the technique is shortly described in the end.

### 2.4.1 Optical microscopy

#### 2.4.1.1 Instrument components

Optical microscope uses a system of lenses to magnify images of small objects irradiated with light. The main components of typical microscopes are presented on Figure 2.9. As presented, depending on chosen illumination path, image can be obtained from the light that is transmitted through the specimen or that is reflected from it. In fluorescence mode usually the second approach is used. Different magnifications are obtained by changing objectives. The field depth (distance between the nearest and farthest plane in focus) can be changed by adjusting aperture diaphragms. The image brightness depends on illumination intensity and exposure time of the camera. The most simple illumination technique in transmission microscopy is called bright field, and it does not require any special filters. In order to enhance contrast between different phases of the specimen, techniques such as dark field (excluding unscattered light), phase contrast or differential interference contrast (DIC) microscopy can be employed. The two latter ones are especially useful in imaging phase changes in transparent specimens [52].

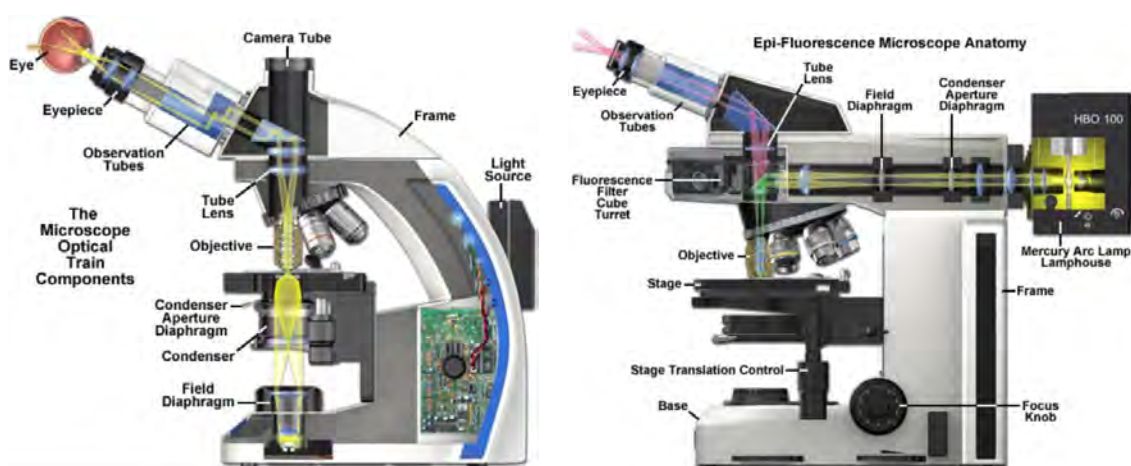


**Figure 2.9:** Components of a typical optical microscope operating in transmission mode (left) and a microscope with equipment necessary for capturing fluorescence images operating in reflectance mode (right) [52].

In order to obtain fluorescence images, a microscope must be equipped with a filter set, which allows to irradiate a sample with light of certain wavelength range, and observe it in another wavelength range at the same time. The illumination must be intense, nearly monochromatic, hence HBO 100 mercury arc lamps are typically used. The drawback of those lamps is that its radiation intensity can be unstable, what may cause problems if one wants to perform quantitative measurements [53].

### 2.4.1.2 Fluorescence and fluorophores

Fluorescence itself, is a phenomena that occurs when absorption of a photon by a molecule (fluorophore) results in transition of an electron to an excited singlet state, and subsequent emission of another, lower energy photon when the electron goes back to the ground state [54]. Therefore, in fluorescence microscopy we irradiate the sample with shorter wavelength and observe the image in longer wavelength.

Fluorophores often contain multiple aromatic rings, but they can be as well planar or cyclic compounds with several  $\pi$ bonds, so most dyes fulfill this condition. The absorption and emission wavelength vary for different molecules, hence it is important to use appropriate filter sets.

### 2.4.2 Dynamic light scattering (DLS)

DLS is a technique used to determine size distribution profile of suspended nanoscale particles or dissolved polymers. It is based on the fact that a beam of light is scattered in all directions once it hits particles that are small in comparison to its wavelength (hence the size limitation). The intensity of scattered light fluctuates over time because the particles undergo Brownian motion. Autocorrelation function and different mathematical treatments are then employed to extract data about particle dynamics and size distribution. In DLS instrument, a laser beam passes through polarizer, impinges a particle, and light scattered from it is passed through another polarizer to a detector positioned at some specific angle [55]. It is recommended to use several different angles for an analysis, especially when range of particle size distribution is unknown.

Typical output of DLS measurement is a graph of particle population for different diameters. It is worth to note that obtained radius is a radius of a sphere that would move in the same manner as the scatter, and it includes molecules that move with a particle. Thereby the size obtained in DLS can be larger than the one obtained from electron microscope images.

# 3

## Methods

### 3.1 Preparation of microcapsules

#### 3.1.1 Materials

All materials were used as received unless otherwise stated. Poly(methacrylic acid) (PMAA, Polysciences, Mw 100,000) and poly(vinyl alcohol) (PVA, Acros Organics, 95% hydrolyzed, Mw 95,000) were used as dispersants. The oil phase components included dichloromethane (DCM, Sigma Aldrich), PMMA (Aldrich, Mw 350,000), PS (Polymer Source, Mw 5000), PPHA (linear, Sigma Aldrich, Mn 5000-8000), hexadecane (HD, Sigma Aldrich), octamethylcyclotetrasiloxane (OMCTS, Sigma Aldrich), acetone (Sigma Aldrich, analytical grade), Disperse Red 13 (Sigma Aldrich),  $\beta$ -carotene (powder, Sigma Aldrich, >93%, type I), Sudan I (Sigma Aldrich), and lycopene (powder, Sigma Aldrich). For titanium dioxide experiments a rutile-anatase  $\text{TiO}_2$  mixture (Aldrich, 99.9%) or Aeroxide P25 (Aerosil) was used. Water of MiliQ grade has been used throughout experiments.

#### 3.1.2 Procedure

Microcapsules were prepared according to the procedure described by Loxley and Vincent [12] with small modifications. Exact parameters and compositions of different encapsulation batches can be found in Appendix A.

##### *1) Preparation of the emulsion phases*

The aqueous phase of the emulsion was obtained by dissolving the emulsifier (PMAA or PVA) in MiliQ water under vigorous stirring at 85-90 °C, and was cooled down to room temperature prior to use in emulsification. 1 wt% emulsifier solutions were used throughout the project, with the exception of batch 17, where 2 wt% PMAA solution was used. The oil phase was prepared by dissolving the shell material (PMMA, PS or PPHA) and core material (HD or OMCTS) in DCM. In all cases acetone was added to aid emulsification. The ratio of these four components was constant, excluding batch 19 where less polymer was used to obtain thinner capsule walls and batch 22-23 where more PPHA was needed to obtain core-shell structure. When new formulations were tested, no dye was added, to exclude its potential impact on encapsulation process. In other cases Disperse Red 13, Sudan I,  $\beta$ -carotene or lycopene were added for the purpose of release studies. Care was taken to ensure that the dyes won't precipitate during encapsulation, so first their solubility in HD was determined, or in case when complete dissolution was difficult to achieve - a

filtrate of dye-HD mixture was used as a core material. The effect of using excess amount of dye was checked on Disperse Red 13.

#### *2) Emulsification*

The emulsification was carried out using Heidolph SilentCrusher M homogenizer equipped with dispersion tool 22 F or 8 F, depending on volume requirements. The vessel was accordingly a 200ml or 5ml double-necked round-bottom flask, immersed in a water bath to prevent overheating. The volume ratio of oil phase to water was approximately the same for all encapsulations (small variations due to different density or mass of used polymer could occur). The oil phase was added dropwise over approximately 3min to the aqueous phase stirring at 5000 rpm. The rotation speed was further regulated so that appropriate mixing is achieved and no foaming occurs, taking under consideration target size of the capsules. The emulsion was homogenized for 60 min when large-volume setup was used. To check if the time can be reduced, emulsion samples of batch no. 6 were taken for microscopic examinations after 2 and 10 min of homogenization. In the small volume setup, where mixing was worse, the time was extended to 80 min.

#### *3) Solvent evaporation and storage*

Once the homogenization process was over, the emulsion was immediately diluted by pouring it onto gently stirred aqueous phase (1.5 times the amount used in the emulsification step). In most cases the mixture was left stirring overnight in a beaker under a fume hood, what allowed slow evaporation of DCM that should result in less porous shell structure [12]. In batches no. 1 and 21 fast evaporation in rotary evaporator was used instead. Obtained microcapsule suspensions were stored in closed bottles under gentle magnetic stirring or in vials. When PPHA was used as shell material, care was taken to protect it from light during all encapsulation steps and storage.

### **3.1.3 Comments regarding working on small volumes**

Some of the photosensitive polymers, like PPHA, are produced only on a laboratory scale, hence they can be very expensive and available in small quantities. Reducing the material use could be achieved by lowering the emulsion volume or by lowering the oil-to-water ratio. The former was chosen, because changing the ratio would increase the rate of DCM diffusion to the aqueous phase, what could result in phase separation during homogenization. Hence a low-volume setup was built that allowed to use less components comparing to the standard recipe adapted from Loxley and Vincent [12]. Scaling down the microcapsule production was associated with some new problems. The way in which they were managed is described below.

#### *Avoiding contamination*

In order to achieve microcapsule suspensions resembling those produced in large volume setup, it was necessary to pay a special attention to avoid contamination. All the surfaces that the emulsion components have contact with were washed with ethanol and distilled water prior to use and care was taken to not introduce new



contaminants after that. If possible Polytetrafluoroethylene (PTFE) caps were used for the vials with the oil phase. The starting materials for the oil phase were filtered with a filter paper or with a syringe membrane filter compatible with given substance. Attention was paid if there are no precipitates or impurities in the aqueous solutions of PMAA and PVA. If necessary, fresh solutions were prepared.

#### *Accurate weighting and avoiding material loss*

The polymer was weighted on an analytical balance directly in the vial (8 or 20 ml) in which the oil phase was to be prepared. When charges on the powder particles were an issue, a Zerostat 3 antistatic instrument (Sigma Aldrich) was used. To ensure that DCM content is accurate, the vial with oil phase was capped when possible and its weight was controlled before emulsification. For adding the oil phase to the emulsion a glass syringe was used, so that the surface from which DCM could evaporate was minimized at this step. Another advantage of using a syringe is that not much material is left on the walls.

#### *Achieving good mixing during homogenization*

The emulsification required using a smaller dispersion tool and a 5ml pear-shaped flask, which had an irregular shape because of the second neck. The emulsion volume and tool position was adjusted so that a compromise between minimum immersion depth of the rotor and proper mixing conditions is achieved. In case when mixing in the surface region seemed insufficient, a glass syringe was used to transfer this phase closer to the rotor tip. Syringe mixing must be performed with attention to not introduce air to the emulsion, otherwise more foam will be produced. As mentioned in the previous subsection, homogenization time was increased to 80 min to compensate for the worse mixing conditions.

### **3.1.4 Experiments with TiO<sub>2</sub> nanoparticles as emulsifier**

With intention to incorporate TiO<sub>2</sub> on PS microcapsule shells, possibility to use it as emulsifier instead of PMAA or PVA was investigated. The nanoparticles were in form of powders, hence they had to be dispersed in MiliQ water first (at 1 wt%). Initially an anatase-rutile mixture from Sigma Aldrich was used for the dispersion experiments, but it was soon replaced by Aeroxide P25 TiO<sub>2</sub> as sedimentation was slower in the latter one. Dispersion was performed with ultrasonicator (Vibra-Cell, max power 500 W). Different powers and sonication times were tried out - ultimately 20min of sonication at 36% W was used. To avoid instant sedimentation, pH of the mixture was adjusted to be far from isoelectric point with solutions of hydrochloric acid and sodium hydroxide (eventually pH 3 was chosen). Size distribution of suspensions diluted with MiliQ water adjusted to pH 3 was checked on DLS.

Emulsification tests were performed on same volumes of water and oil phases as for production of microcapsules, but without polymer, core material and stabilizer. During homogenization, after the oil phase was added, pH was adjusted to 6, close to

the isoelectric point. Since those experiments were not successful, ODPA was added to the oil phase in order to anchor  $\text{TiO}_2$  to the droplet surface (acetone and ethanol had to be added to aid dissolution of ODPA in DCM). At last an attempt to modify the particles with ODPA was performed by following the procedure described by Demina *et al.* [56].

## 3.2 Characterization with optical microscopy

### 3.2.1 Equipment

Optical microscope equipped with 10x, 40x, 50x and 100x objective lenses was used throughout the project in transmission mode. Bright field (BF), dark field (DF), differential interference contrast (DIC) and fluorescence modes were employed to create the images. For fluorescence HBO 100 lamp was used with 38 HE, 20 HE or 49 Filter Set (Zeiss).

### 3.2.2 Methods

For each encapsulation batch images of the emulsion and microcapsule suspension were taken in BF. In most cases fluorescence images were taken as well to visualize the dye or polymer fluorescence (if present). Images of the emulsion samples were taken shortly after it was homogenized and diluted, while those of capsule suspensions were captured after solvent evaporation, usually the day after preparation of emulsion.

Attention was paid to microcapsule morphology and to location of the encapsulated dye. Size distribution of the emulsion droplets and capsules was only roughly estimated by looking at representative images taken with 10x and 40x objectives. No software was used to extract more exact data, because the main purpose was to identify problems such as bad mixing and to decide whether some parameters must be changed to obtain capsules of the target size.

For the purpose of release studies microcapsules in a dry form were also imaged (see section 3.3.1). No cover glass was used in this case, because of a repulsion. Different filters, acquisition parameters and postprocessing options were tested to visualize the released oil and capsule morphology. It was difficult to interpret the images of dry capsules, so the process of suspension drying was registered in time series experiments to gain more insight.

## 3.3 Release studies

### 3.3.1 Preparation of dry microcapsules monolayer

To investigate the reaction of dry capsules to a release trigger with light microscopy, it was convenient to have them in one plane, separated from each other. Initially it was planned to use spincoating, a method commonly used to create thin films, to achieve the desired effect. A spincoater was employed to spin a microscope slide, so that a drop of capsule suspension placed at its center spreads by centrifugal force. Different spinning times, angular speeds and acceleration modes were tested.

An alternative method was to simply place a drop of suspension on a glass slide, tilt it so that the liquid spreads on the surface and leave it to dry. This procedure was preferred because it is more gentle for the capsules, gives direct control over their placement on the slide, and enables one to observe the drying process under a microscope.

Microcapsules have a tendency to aggregate when the water evaporates regardless of method used to prepare the monolayer. To reduce this problem the suspensions were diluted with MiliQ water prior to dropping on the slide. Most often one part of original suspension was diluted with eight parts of MiliQ in this work.

The water from suspensions smeared on the glass slides seem to evaporate in few minutes, but to ensure that there are no remains on the surface, the samples were left to dry for at least 30 min before experiments with UV irradiation.

### 3.3.2 Triggered release investigation

Investigation of the release with light microscopy was performed on PMMA, PS and PPHA microcapsules with dissolved Sudan I or lycopene in their HD cores to aid visualization. Initially Sudan I was the preferred dye because of its good solubility in HD, therefore it was encapsulated in PMMA and PS batches. Because of concern that it can affect the response of polymer shells to UV, it was replaced with lycopene for the PPHA microcapsules. An UV experiment was performed on PPHA capsules without a dye in the core as well.

To obtain reference images of core release, the shells were fractured by application of an external pressure or by dropping methanol on the monolayer slide. More detailed descriptions of experiments with different triggers can be found below.

#### *Mechanical crushing*

At the beginning an attempt to fracture microcapsules with a cover glass or needle was performed, but this turned out to be difficult. Finally, the particles were crushed with a round tip of a clean glass rod. The boundary where crushed and unaffected capsules meet was observed to see how released oil should look like.

#### *Methanol*

The reaction of microcapsules to methanol was investigated by imaging the same spot of prepared monolayer before and after a drop of methanol was placed on it. Methanol swells the polymer and evaporates almost immediately, thereby it was expected to trigger the release without applying external pressure by mechanical means.

#### *Ultraviolet light*

HBO 100 W/2 lamp (Osram) was employed to irradiate the dry microcapsules with UV. Some of the lamp emission output lies in infrared region, so to prevent overheating of the sample, the light was passing through a water filter first. The photon density was approximately  $5 \cdot 10^6$  photons per  $\text{cm}^2$  per second, and the energy density was  $600 \text{ W/m}^2$  [7]. Chosen spot of microcapsule monolayer was imaged, irradiated for a certain amount of time and imaged again. If necessary, it was irradiated further and changes in the sample were monitored in the same manner. The total irradiation times varied from 30 minutes to 10 hours for different samples. The choice was primarily based on degradation rate of corresponding polymer films, and in some cases the time was extended because no response could be observed.

# 4

## Results and discussion

### 4.1 Formulation of reference microcapsules with PMMA shells

In order to study the release from microcapsules using light microscopy, it was convenient to dye the encapsulated core oil and to tune their size so that they are big enough to see under 50x objective, and small enough to have thin shell walls that could be easily disintegrated after UV irradiation. Different dyes, dispersants and emulsification parameters were used to obtain desired effects. Influence of different components (dyes, dispersants and core oils) on microcapsule morphology was also examined. Finally, optimization of production with small volume setup was performed, to enable synthesis of microcapsules from small amounts of available UV sensitive polymers. All these modifications were performed in initial stage of the thesis on microcapsules with shells made of commonly used PMMA. The results of using different components and production parameters are summed up in this section.

#### 4.1.1 Dyes

Three different dyes were used to aid visualization of the HD cores of PMMA capsules: Disperse Red 13,  $\beta$ -carotene and Sudan I. In the latter stage of the project also lycopene was used to dye the core of PPHA capsules (see Section 4.2.2).

##### *Disperse Red 13*

Disperse Red 13 used in first encapsulations was added in quantity sufficient to give light red color to the oil phase of the emulsion. Contrary to our expectations, the color was not visible on the bright field microscope images of obtained microcapsules (See Figure 4.1a). In another batch Disperse Red 13 was added until the oil phase had color of a dark wine, so that its solubility in HD could be exceeded. The effect was that a slightly pink color could be visible near the edges of big microcapsules (Figure 4.1c). It was clear at this point that bright field microscopy will not be enough to visualize the dye in thin layers of oil leaking from the capsules, so fluorescence mode was used for this purpose. As shown on Figure 4.1d, intense signal from the dye could be observed on fluorescence images with excess dye.

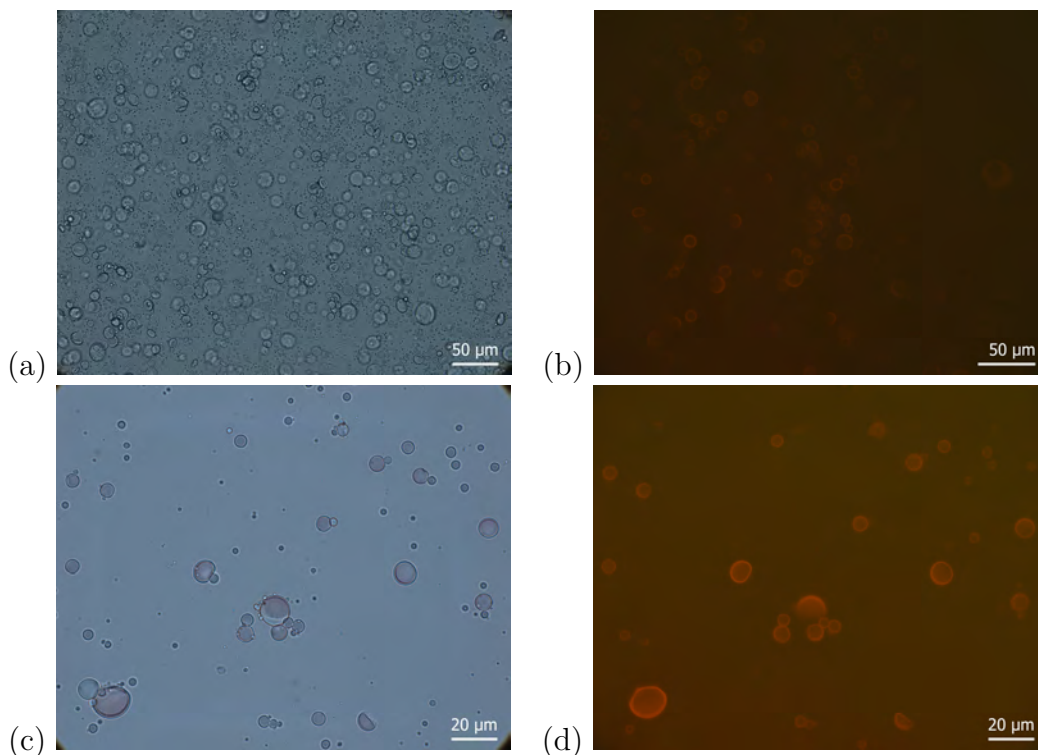


**Figure 4.1:** Bright field (left) and fluorescence (right) images of microcapsules with Disperse Red 13 added in small amount (a,b) and in large amount (c,d).

#### *$\beta$ -carotene*

Because of the tendency of Disperse Red 13 to migrate to the shell, microcapsules with  $\beta$ -carotene were prepared. This time necessary amount of the dye was weighed on analytical balance to ensure that the solubility limit for similar to HD hexane (1.1 g/l according to the manufacturer [57]) is not exceeded. A slightly lower concentration was used (1 g/l of HD) since hexane is a smaller molecule and hence better solvent than HD. As expected, long hydrocarbon chain in  $\beta$ -carotene structure makes the molecule hydrophobic enough to remain in the core - not in the shell (see Figure 4.2). The drawback of using  $\beta$ -carotene was that the fluorescence intensity of the dyed oil was rather low at used concentration.

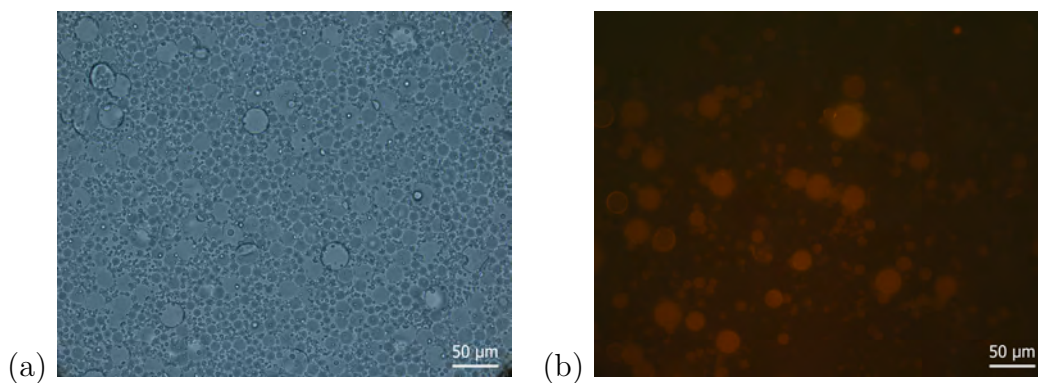


**Figure 4.2:** Bright field and fluorescence images of microcapsules with  $\beta$ -carotene.

*Sudan I*

Sudan I was chosen for further experiments because another group achieved intense core color with it. First the dye was dissolved in HD to ensure that the value given in literature (3.7 g/l of HD at 25°C [58]) is correct. A solution of concentration 3.3 g/l was obtained after a night of vigorous stirring in HD. The image (Figure 4.3a) of microcapsules produced with this dye confirms that Sudan I does not have a significant tendency to migrate to the shell, but if its amount doesn't exceed solubility limit in HD, the intensity of the color is not high enough to visualize leaking oil without fluorescence (it has to be considered that once the oil leaks out, the layer would probably be too thin to see any color at all in the bright field mode). Nevertheless, high intensity of fluorescence signal from capsules with Sudan I (Figure 4.3b) seemed to be enough for the purpose of release studies, therefore this dye was used for most encapsulations in this project.

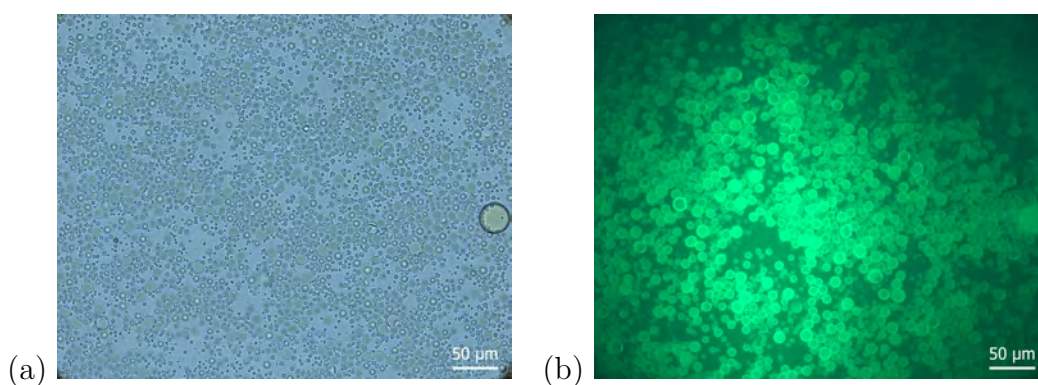


**Figure 4.3:** Bright field and fluorescence images of microcapsules with Sudan I.

*Lycopene*

For the reasons discussed in Section 4.5.1, the batch of PPHA microcapsules was prepared with lycopene instead of Sudan I. The value of solubility in hexane (1 g/l at 14°C [59]) found while doing a basic internet search was promising, considering that lycopene could give a higher fluorescence intensity than  $\beta$ -carotene. Nonetheless it was difficult to dissolve lycopene even below concentration of 0.1 g/l both in HD and in hexane. Authors of an article found later on also reported problems with dissolving lycopene in hexane at concentration of 0.1 g/l (eventually they dissolved 0.008 g/l)[60]. Increasing the solution temperature could aid dissolution, but then its degradation or precipitation during encapsulation could occur. Therefore a filtrate of HD/lycopene mixture was used as the core component of the PPHA capsules. Obtained solution had a very pale yellow color which did not foreshow fluorescence signal that would be strong enough to visualize the core. Since PPHA is fluorescent as well, it was impossible to distinguish signals of the shell and core using available equipment (see Figure in Section 4.2.2).

##### *Effect of excess dye in the core*

It could be noticed that some of the capsules with large amount of Disperse Red 13 had irregular shapes or were acorn-like (Figure 4.4). It is likely that the large amount of dye with the tendency to migrate to o/w interface lowered the interfacial tension in those cases. However, it is not clear if excess of the dye affected other irregularities in the morphology, since this batch was left for too long at DCM evaporation step and water evaporated from the suspension as well (the capsules were redispersed with adequate amount of MiliQ before microscopic examination).

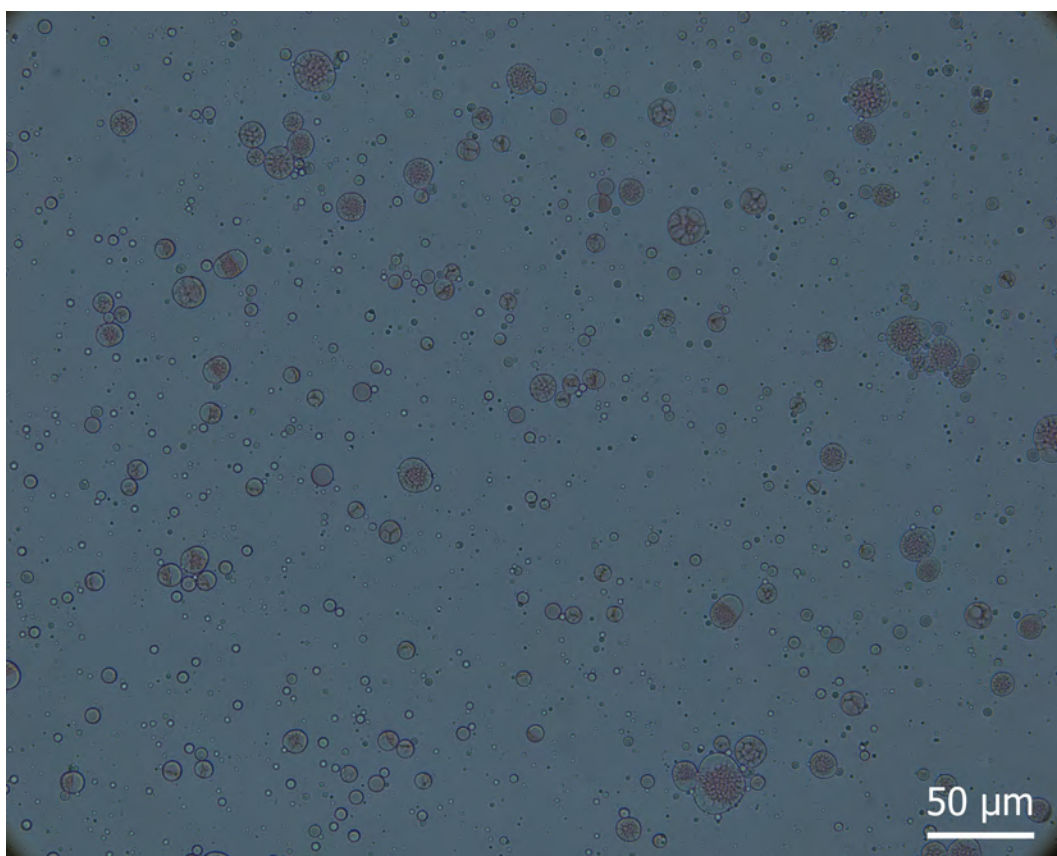


**Figure 4.4:** Particles from the batch with large amount of Disperse Red added to the oil phase - region of suspension where acorn-like particles were present.

In an early test of small volume setup, it happened that microcapsules with Sudan I had an intense yellow color. It is very unlikely that it was the effect of settings used to capture the image (different parameters were tested before and similar intensity was not obtained), indicating that the dye concentration could be higher than 3.3 g/l in this case. Some of these particles had morphologies resembling those from excess Disperse Red 13 batch, however it is not clear if acorn particles were present (Figure 4.5a). Similar particle shapes were also observed in another small volume test, in which obtained capsules did not have such intense color (Figure 4.5b). Possibly impurities could be responsible for this effect.



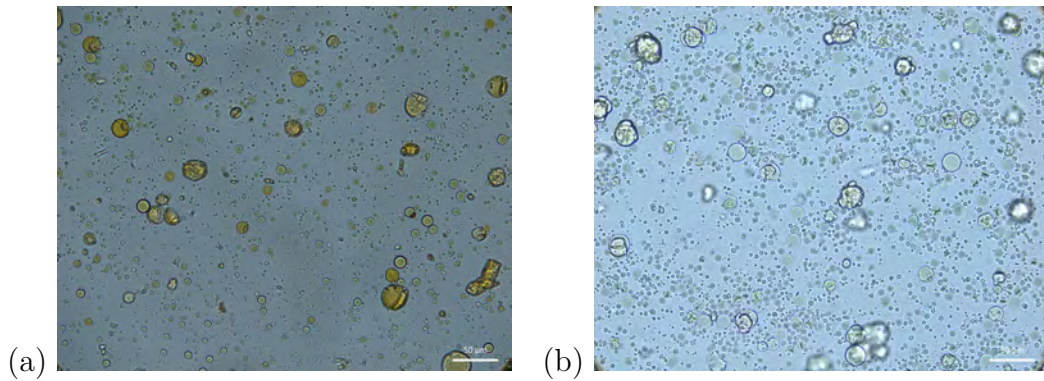


**Figure 4.5:** Microcapsules with possibly higher ( $>3.3$  g/l of HD) concentration of Sudan I (a) and with impurities in the emulsion (b). The scale bar is 50 m.

Regardless of influence of excess dye on microcapsule morphology, it is better to avoid exceeding its solubility limit in core oil. When concentration of the dye is high, the probability that it will affect the response of the polymer to UV is increased. As mentioned in Section 2.7, dyes and pigments are used to stabilize polymers against photooxidation. It is suggested in literature that the conjugated bonds responsible for the color in compounds such as  $\beta$ -carotene and lycopene (or any chromophores in general) are also giving them antiradical properties [61]. Thereby they could hinder shell decomposition in systems where radicals play a role in polymer degradation.

#### 4.1.2 Core materials

Some microcapsules with HD core had indentations in their shells, which were also observed by other groups and assigned to gradients in interfacial tension during encapsulation [12]. The blueberry-like morphology is captured on Figure 4.6a. Since using OMCTS as a core has proven to give good results in previous studies conducted in the department, one microcapsule batch was prepared with this oil and PVA as dispersant. No blueberries were observed in this case and it seemed like the surface of capsule walls is smoother (Figure 4.6b). The overall difference in microcapsule suspension appearance was not significant enough to choose OMCTS over HD, so the latter one was used for all other encapsulations.

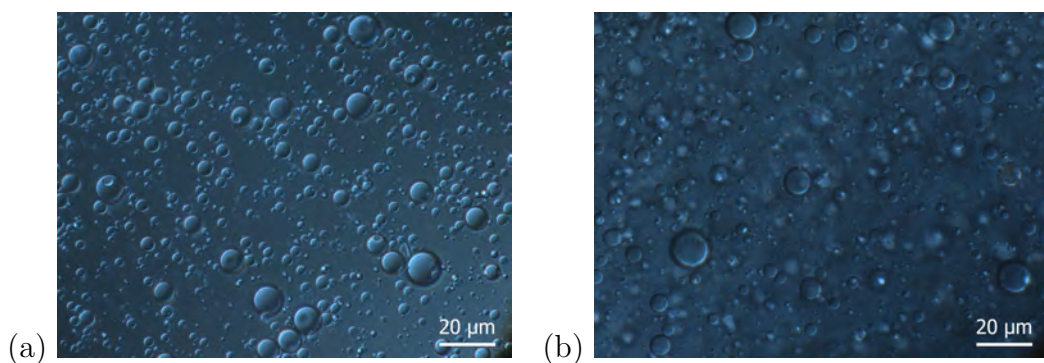


**Figure 4.6:** Microcapsules with HD cores with visible indentations (a) and microcapsules with OMCTS cores (b).

### 4.1.3 Dispersants

PMAA and PVA in form of 1% solutions in MilliQ water were used as dispersants throughout the project. The difference between them could be noticed at the emulsification step, especially in the small volume setup, where problems with mixing occurred. Emulsions with PVA appeared uniform shortly after addition of the oil phase, while when PMAA was used it happened quite often that big oil droplets would not disperse without aid from syringe mixing. A thin transparent layer at the PMAA emulsion surface was also observed in the small volume setup. Moreover a white precipitate was flowing on the emulsion surface after each homogenization with PMAA. On the other hand, when PVA was used as emulsifier, clearly more foam was formed than in case of PMAA (at same rotation speeds). Those observations suggest that PVA migrates faster to the o/w interface or/and binds more strongly to it. Microscopic images of obtained emulsions (Figure 4.7) show that droplets stabilized with PVA are much smaller than those obtained with PMAA. Moreover fast droplet coalescence in PMAA sample was observed under a microscope, while in PVA droplets this phenomena occurred only in small extent.

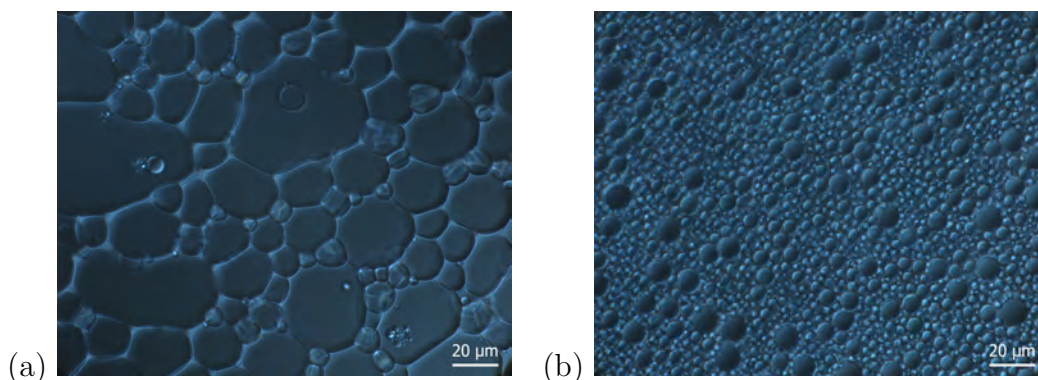


**Figure 4.7:** DIC images of emulsion stabilized with PMAA (a) and PVA (b) captured shortly (<15min) after homogenization.

Even though stability of emulsion with PMAA was bad comparing to the one with PVA, encapsulation was successful in both cases, as can be seen on Figure 4.8.

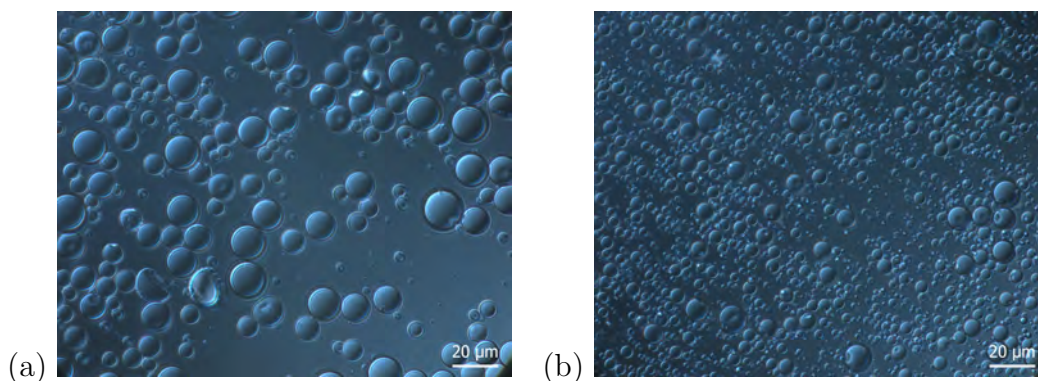


**Figure 4.8:** DIC images of microcapsules stabilized with PMAA (a) and PVA (b).

In fact, microcapsules with PMAA seemed to have less blueberry-like morphology defects. That is consistent the hypothesis that presence of indentations is related with spreading conditions during production [12], since PVA seemed to be more efficient in decreasing interfacial tension. However, no acorns were observed in PVA batch, contrary to the results of spreading conditions calculations presented in the article by Loxley and Vincent [12].

However PMAA gives satisfactory results when it comes to the morphology, there were some limitations to its use. First of all, it couldn't be used for PPHA capsules due to its acid nature (see Section 4.2.2). Secondly, it turned out at some point that Sudan I is soluble in the aqueous phase with PMAA, what is problematic for the release studies. PMAA and PVA microcapsule suspension filtrates were compared with the naked eye - both appeared transparent, but the former one clearly had a yellowish color while the other one did not. Fluorescence microscopy observations suggested that small quantity of the dye could be present in the PVA filtrate as well, however that should be confirmed spectrometrically (it was not as the PVA suspension was lost before the experiment).

#### 4.1.4 Rotation speed and emulsification time

Obviously increasing the rotation speed of the homogenizer led to decrease in emulsion droplet size and improved the mixing in a vessel, but at the same time more foam was produced. The optimal rotation speeds used in different encapsulations are given in Appendix A.

The procedure given in Loxley and Vincent [12] article involves 60min of emulsion homogenization, what seems to be quite a long time. In order to check if the emulsification step can be shorter, samples of homogenized emulsion were taken for microscopic examination 2min, 10min and 60min after addition of the oil phase. The results are shown on Figure 4.9. The big spheres spheres are most likely air bubbles, and were observed in the "60min" emulsion as well. It could be noticed that longer homogenization time gives smaller droplets and more narrow size distribution. Observed difference between the "2min" and "10min" samples seemed more significant than the difference between "10min" and "60min" droplets.

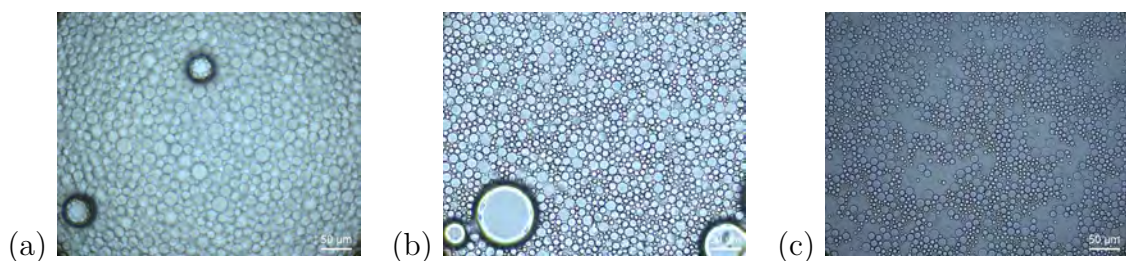


**Figure 4.9:** Emulsions sampled after 2min (a), 10min (b) and 60min (c) of homogenization.

Even longer homogenization time was necessary when small emulsion volumes were produced, as the mixing was often not sufficient in the small setup. Figure 4.10 shows

the difference between 60min and 90min of emulsification. The images suggest that the additional homogenization time gave more narrow size distribution and smaller droplet size. Subsequent small volume batches were emulsified for 80-90min with satisfactory results.

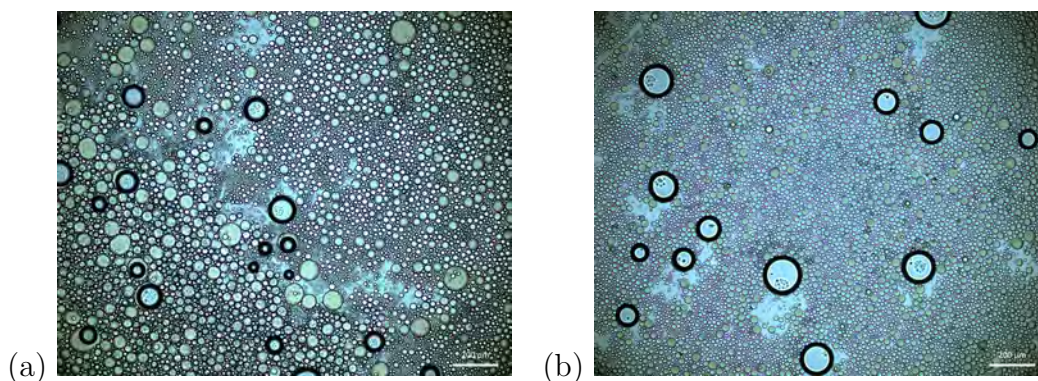


**Figure 4.10:** Emulsion produced in small volume setup after 60min (a) and 90min (b) of homogenization. The big spheres that are not yellow can be air bubbles.

#### 4.1.5 Optimization of production in small volume setup

As indicated in 3.1.3, special measures had to be taken to obtain good emulsion in the small volume setup. The minimum immersion depth of the rotor made it difficult to add the oil continuously in small (dropwise) portions in available glassware. No good results were obtained when the oil was added in few larger portions during pauses in homogenization, so a small two-necked vessel had to be ordered. The beaker had irregular shape due to the second neck, so that good mixing was difficult to achieve. Implementation of syringe mixing and increasing the homogenization time (Section 4.1.4) fixed this problem to some extent.

Control over accurate amounts of oil phase components was also an issue. High vapour pressure of DCM is problematic when automatic pipetting is used. A significant amount of the solvent (nearly 20% of volume used here) can leak out from the pipette, even if the transfer from bottle to beaker is done very fast. In the end, even more DCM can be lost when contribution from evaporation at all stages is included. Therefore during preparation of the oil phase the content of DCM should be checked on analytical balance, with care to avoid bias from the stirring magnet or electrostatic forces. Weighting the oil phase components directly in a vial in which they are further mixed and keeping it capped whenever possible helps to minimize the material loss. Also using a glass syringe to drop in the oil phase to the emulsion turned out to be a very good way to avoid polymer remains on the glassware and DCM evaporation.

As mentioned in 4.1.1, impurities in the small volume emulsion could notably affect microcapsule morphology. Irregular particles, some of which resembling acorns, appeared in early tests even when no dye was used, indicating that interfacial tension could be in some way reduced by adsorbed impurities. Improvement was observed

as possible sources of contamination were eliminated. HD and acetone were filtered through appropriate syringe or paper filter, glassware and dispersion tool were washed with ethanol or acetone and then with distilled water prior to use, and care was taken to keep the work station clean. The effect of implementing all improvements described in this section is presented on Figure 4.11

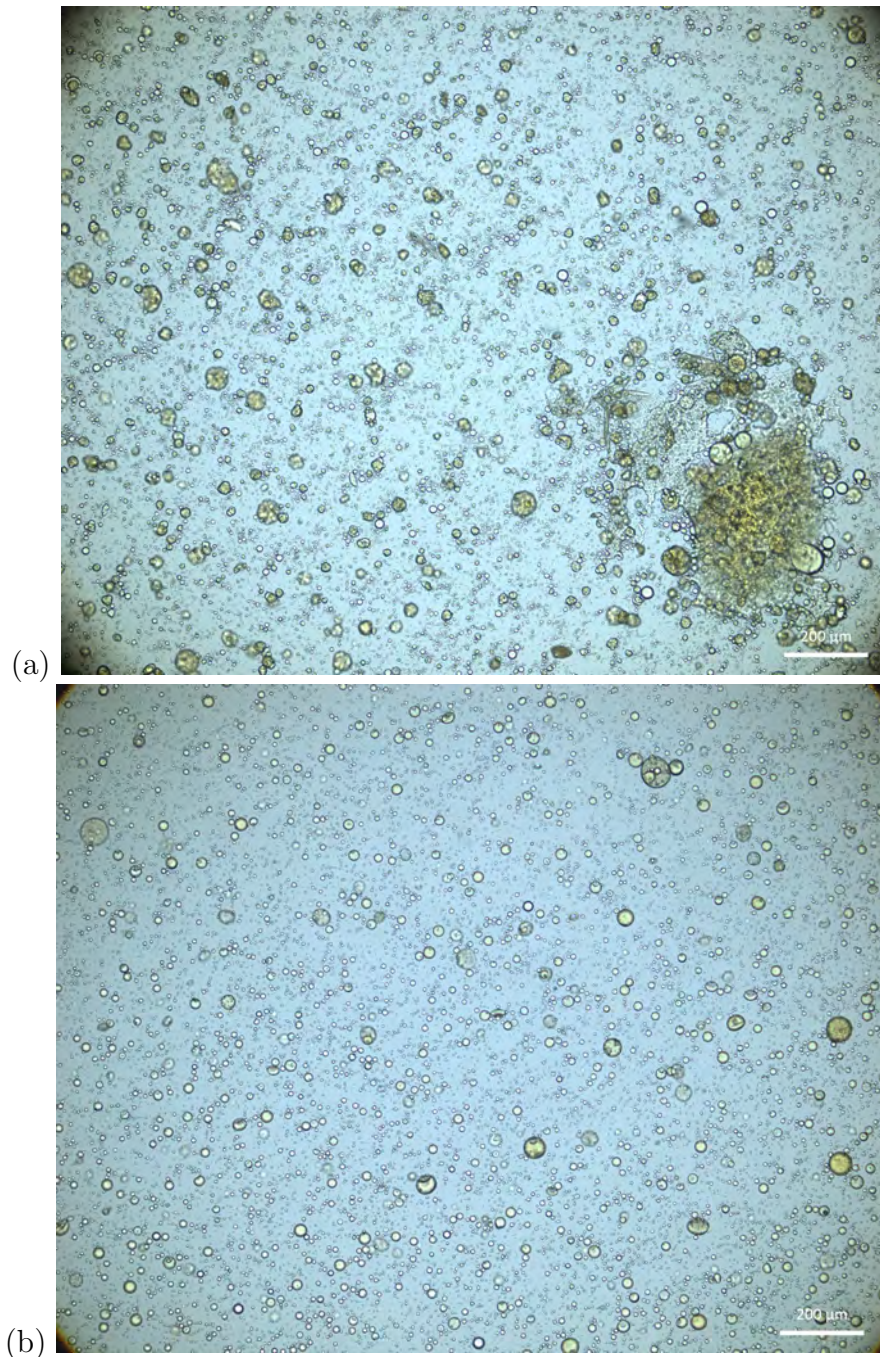


**Figure 4.11:** Suspension of microcapsules with Sudan I obtained at an early stage of small volume setup tests (a) and after optimization of the production method. The scale bar is 200  $\mu\text{m}$ .

## 4.2 Formulation of microcapsules with UV sensitive components

Two approaches to prepare microcapsules that could release the core after exposure to UV were tried out. The first one involved using PS shells that could photooxidatively degrade under UV irradiation. To make the shells more prone to disintegration capsules with thinner walls were produced. In intent to incorporate photocatalytic  $\text{TiO}_2$  particles on the shell surface, the possibility to prepare pickering emulsions with them was investigated. The second approach was to use low ceiling temperature polymer (PPHA) as the shell material. Both polymers exhibited degradation under UV in a parallel thesis work conducted in the department [7].

### 4.2.1 PS shells, thinner shell walls and $\text{TiO}_2$ as emulsifier

#### 4.2.1.1 Microcapsules with PS shells

PS shell was expected to degrade more easily under UV irradiation than PMMA, hence microcapsules with this polymer were prepared in the small volume setup, following the same procedure as for the reference PMMA capsules. Encapsulation was successful for systems stabilized with 2% PMAA, 1% PMAA and 1% PVA. 2% PMAA solution was initially used following the recipe from another article [19], and as can be noticed on Figure 4.12a, many small particles were obtained, but the size distribution was not improved (effect of bad mixing in small volumes). Comparison with the 1% PMAA batch would not be credible, as homogenizer stopped working during emulsification in this case (but microcapsules were obtained).

A batch with thinner shell walls (about 100 nm instead of 500 nm on average) (Figure 4.12b) were obtained by adding less polymer in the oil phase. Because of the reasons discussed in Section 4.1.3 PVA was used instead of PMAA. It seemed like thinner walls does not affect the appearance of microcapsule suspension under light microscope.

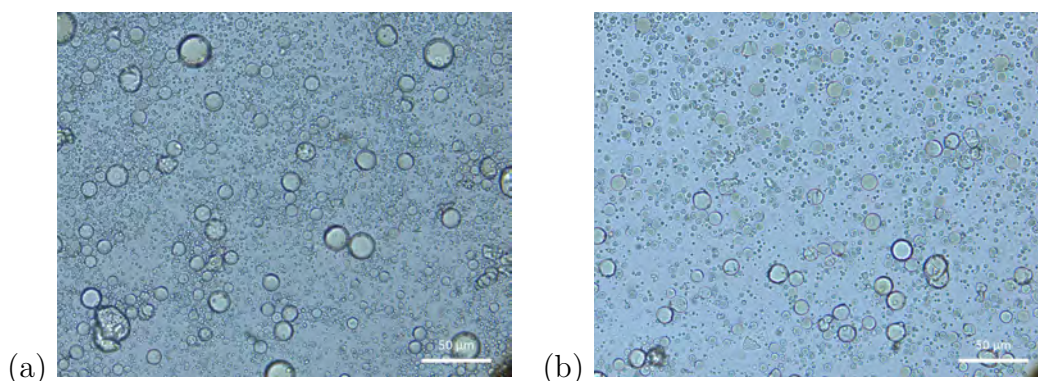


**Figure 4.12:** PS microcapsules with Sudan I with standard shell thickness (a) and with thinner shells (b).

#### 4.2.1.2 Pickering emulsion with TiO<sub>2</sub>

Aqueous dispersion of TiO<sub>2</sub> nanopowders to primary particles was not achieved. Both rutile-anatase mixture from Sigma Aldrich and Aeroxide P25 dispersions were opaque white and sedimented rapidly after sonication. The former one seemed to sediment more rapidly, hence only P25 was used for further experiments. After adjustment of pH to 3, the suspension remained stable for longer time - apparent sedimentation could be observed after an hour approximately. However, even then the dispersion was rather opaque and flocculates could be observed under optical microscope, what indicates that size of the aggregates was not even close to primary particle size (20 nm according to the producer). Results of DLS measurement showed that the mean particle size for 90° angle was 175 nm. An explanation for this can be that the particles chemically bonded together in the manufacturing process forming irreversible aggregates, as pointed out by Zhang *et al.* [62], who studied stability of commercially available metal oxide nanopowders in water and met the same problems.

Emulsification with TiO<sub>2</sub> as stabilizer was not successful. Changing pH to 6 during homogenization or adding ODPa to the oil phase did not help to obtain small droplets, even at very high rotation speeds. It could be observed soon after homogenization that the mixture separates into three phases: a region of big (approximately 1 mm) droplets separated with the nanoparticles at a bottom of the flask, a white region of sedimented nanoparticles in the middle and a more transparent region of suspended particles near the surface. This indicates that aggregates were too big. Microscopic examination confirmed that proper emulsion was not obtained (see 4.13). Emulsification with particles modified with ODPa was not performed, however it could give more insight on whether unsuccessful emulsification was a result of too big particle aggregates or their hydrophilicity.



**Figure 4.13:** Effect of attempt to form Pickering emulsion with TiO<sub>2</sub> nanoparticles.

### 4.2.2 Microcapsules with PPHA shells

Production of PPHA microcapsules couldn't be performed with PMAA dispersant, because measurement with a pH-meter showed that 1 wt% solution has pH 2.8, what could be too low for the acid-sensitive polymer. Therefore, worse in terms of spreading conditions PVA had to be used (pH 6 for 1 wt% solution). Using the standard recipe used for other encapsulations resulted primarily in acorns, but when the mass ratio of polymer to core oil was increased from 0.66 to 1, most particles had core-shell structure, what can be noticed under optical microscope because the polymer is fluorescent (see Figure 4.14 a, c). This is consistent with findings of Tang *et al.* [63], who reported that core-shell PPHA microcapsules were obtained when ratio was higher than 1, whereas acorn particles were obtained when the ratio was 0.88 or 0.75. Contrary to their results, fast evaporation of volatile solvent was not necessary for proper encapsulation. In fact, it seemed like there are more acorn particles in the batch where DCM was rotary evaporated (Figure 4.14 b) than in the one where slow evaporation under fume hood was performed. The difference in results can arise from using different equipment or using cyclic PPHA by the other group, whereas here the linear polymer was used.

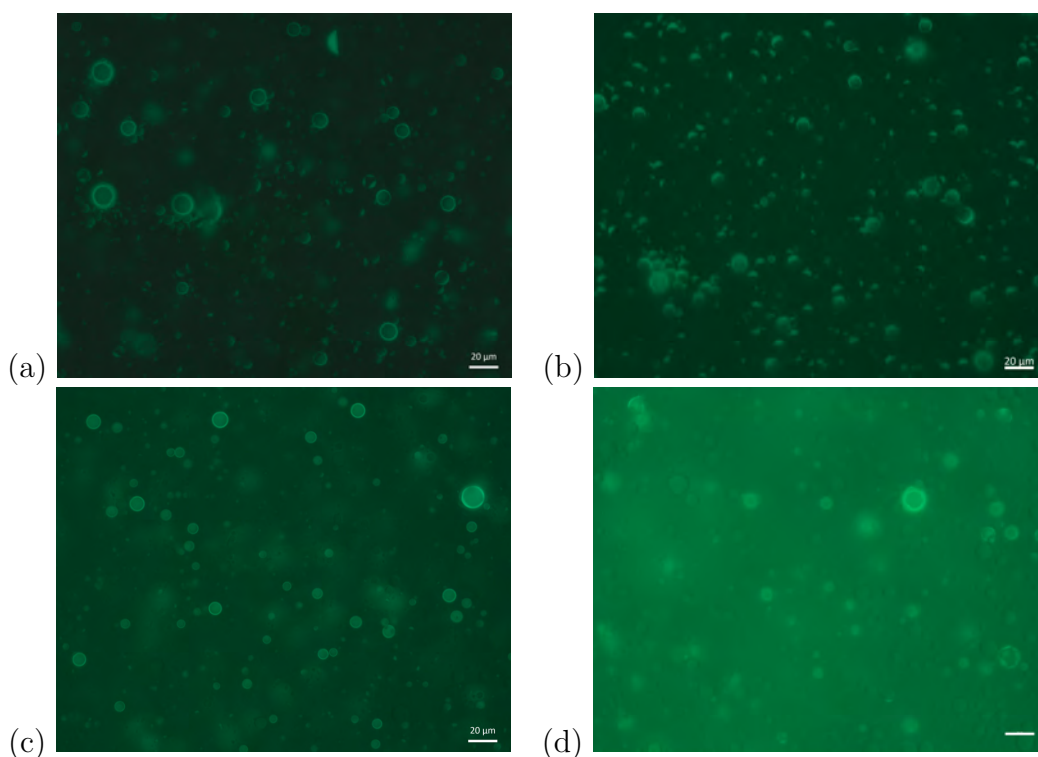


**Figure 4.14:** Fluorescence images of microcapsules with PPHA shells: standard recipe (a), batch where DCM was rotary evaporated (b), batch with higher polymer-core oil ratio (c), batch with lycopene (d). The scale bar is 20  $\mu\text{m}$ .

The recipe with which successful encapsulation was done (more polymer, slow evaporation) was used to produce microcapsules with lycopene dye in the core oil (Figure 4.14 d). This batch appeared to have slightly more acorns, however it is not clear why. It could be a consequence of dye precipitation, since it was problematic to



dissolve it in HD and ultimately a filtrate was used as the core material. On the other hand, the concentration of the dye was so low (the color of the filtrate was barely visible), that it seems unlikely that this explanation is valid. Other factors, such as impurities could cause the effect.

### 4.3 Using optical microscopy for characterization and visualization of released core materials

Optical microscopy was used for characterization of emulsions, suspensions and dry capsules, as well as for release studies. Images obtained with 40x and 100x objectives can be used for assessment of size and morphology of microcapsules in suspension. 10x objective is better for approximate estimation of size distribution and checking for presence of impurities. Because size and size distribution was not the main subject of this study, there was no need to use image analyzing software to obtain more accurate information about them. The fluorescence mode was useful to image core-shell structure of PPHA capsules (see 4.2.2) and to visualize dyed core oil for release experiments. However, mechanical crushing tests (see 4.4) showed that sometimes the leaking oil can be seen in bright field mode as well, so it can be reconsidered if the dye is indispensable for release studies. The dry microcapsules couldn't be imaged with 100x because it is an immersion objective, and here no cover glass was used (it was repulsed from the dry surface). 50x objective was employed instead, since it was optimized for applications where no cover glass is present.

It should be pointed out that it is easy to draw wrong conclusions from microscopic images, especially when the examination technique is not refined for given case yet. To begin with, the distribution of species on the microscopic slide can be very uneven regarding size and morphology of capsules, so finding representative spot is very important. Secondly, morphological defects such as wrinkles or indentations often become visible only after adjustment of diaphragm opening or when DIC mode is used. When it comes to suspensions, it could also be problematic to distinguish between core-shell particles and gas bubbles or complete phase separation of core and polymer. Moreover, flocculate of a small and big particle can look like a blueberry particle. In such cases fluorescent mode or observation of drying suspension can be helpful. At last, while imaging release in a dry state, the field depth may not allow to have both capsule surface and released actives in focus. Z-stacks with a software such as ImageJ or Helicon Focus could distort the appearance of the capsule morphology if not used skillfully, but a good practice is to always capture images of two focus planes for given spot.

When using fluorescence mode, one should keep in mind that some features, become visible after manipulation of histogram data. Parameters such as exposure time of the camera play a role as well. Furthermore, fluorophore bleaching was observed for all dyes and for PPHA shells, so automatic mode should be used to reduce the time of sample exposure to the fluorescence lamp. It is also important to take account of the reaction of fluorophores to UV (see section 4.5). At last, the instability of

the HBO lamp mentioned in 2.4.1.1 can affect the fluorescence intensity signal. All those factors would have to be considered to perform quantitative measurements based on extraction of data from fluorescence images.

In general, the optimal strategy would be to first find good hardware settings for given system, save them and then use automatic options for the imaging. If possible, the images should be stored in RAW files, so that if necessary they can be processed later on to enhance visualization of initially missed features. Finally, different settings and postprocessing options should be used to check for presence of fluorescent species in microcapsules without dye prior to drawing conclusions from images containing it.

### 4.4 Methodology for studying the release from dry microcapsules

The most convenient way to prepare a monolayer of dry microcapsules was to simply drop a diluted suspension (1:8 dilution with MiliQ works well) on a tilted microscope slide and leave it to dry. They will be in one plane after few minutes, but their appearance may change as remains of water evaporate from their surface, so it is better to wait about 30 min before imaging. Spincoating gives comparable results, however it can potentially damage the capsules and it seemed like there are more aggregates. Another advantage of "drop and leave to dry" method is that, contrary to spincoating, it allows to control the amount of suspension on the slide, what could be useful for quantitative measurements of released actives.

In order to image the same capsule before and after trigger event, it should be imaged with 50x and 10x objective. If the position of the region is marked on microscope slide edges, it is easy to find the image matching the one from low magnification. Then the spot matching higher magnification can be quickly found as well. Noting the position from scale bar on the microscope stage was helpful as well. Later experiments with UV irradiation (4.5.2) suggested that one should also look for oil leaks outside the initially assumed region of interest.

To obtain reference images of how release of cargo on the solid surface should look like, swelling the polymer with methanol or mechanical crushing can be performed. Dropping methanol on PMMA microcapsules with Sudan I dye resulted in their collapse and reduction of fluorescence intensity inside them, but no oil leaks were observed (Figure 4.15). Possibly that is because the core material with the dye was dispersed over a large area by the methanol drop.

Inducing the release by mechanical means must involve applying relatively high pressure - the capsules were not affected when they were pressed with a cover glass. Tip of a glass rod had to be used to cause oil leaks, but then it was difficult to capture the same spot before and after crushing. The difference between crushed and not crushed region of capsules can be observed on Figure 4.16.

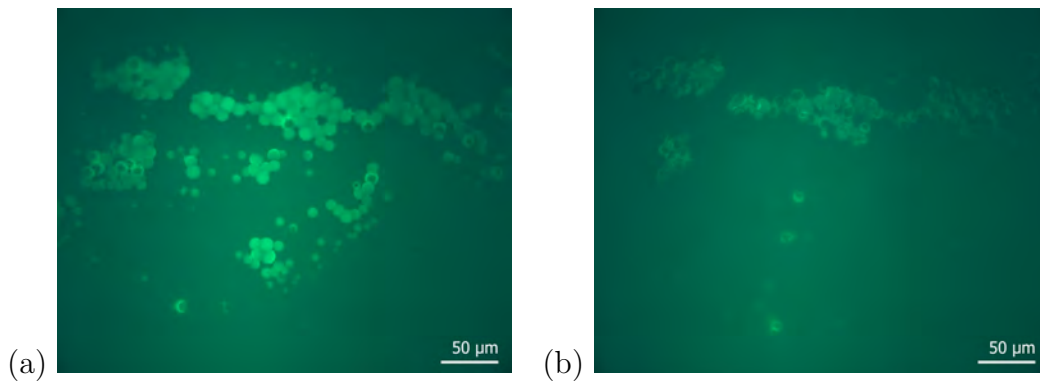


**Figure 4.15:** PMMA microcapsules with Sudan I before (a) and after (b) adding a drop of methanol.

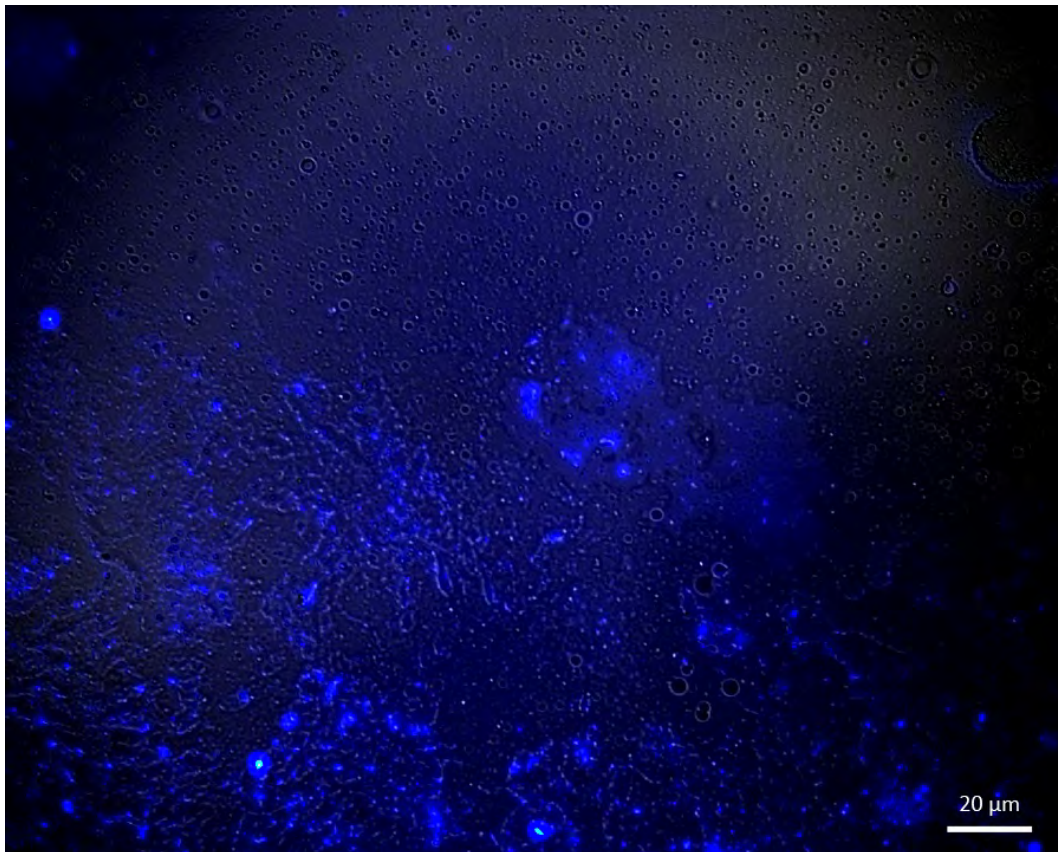


**Figure 4.16:** Image of the boundary between mechanically crushed (bottom) and unaffected (top) region of PS microcapsules with Sudan I, obtained by superimposing bright field and fluorescence image.

Interestingly, the interior of PS microcapsules on which the mechanical crushing test was performed seemed to be not fluorescent until they were damaged. More experiments would have to be performed to be sure that this is the case and to check if similar phenomena can be observed in microcapsules with other shell materials. If the dye fluorescence signal is screened by shell material, it could be an important information for interpretation of the UV triggered images.

## 4.5 Response of microcapsules and their components to UV

UV irradiation experiments were performed on PMMA (both PMAA and PVA stabilized), PS and PPHA microcapsules with encapsulated dye. For the first two it was Sudan I, but because of its reaction to UV light (Section 4.5.1) it was replaced with lycopene for the PPHA batch. The irradiation times were comparable to those that resulted in degradation of the polymer films [7], but as shown in the following subsections, no signs allowing to definitely state that release comparable to this from methanol or mechanical crushing tests was observed. However, the methodology for capturing images of dry capsules was not fully developed when most of the UV experiments were performed. Perhaps if they would be repeated using all recommendations from Section 4.3, different results would be obtained.

### 4.5.1 Sudan I

Before moving on to results of PMMA and PS microcapsules irradiation, it should be emphasized that fluorescence intensity of Sudan I, encapsulated in those batches, increases after exposure to UV light. Similar phenomena have been reported for different fluorophores in literature [64], [65]. The increase has been observed on images presented in following subsections, thus additional experiments were performed to investigate time dependence of the phenomena (Figure 4.17) and to confirm that the dye is responsible for the observed effect (Figure 4.18). It can be noticed that fluorescence of small microcapsules was not even visible before irradiation with UV. Interestingly, the enhanced fluorescence signal persisted even after many days of storing the sample in darkness. Also, it seems like the color tone of the dye in HD is changed after UV. Those observations could mean that a stable product with higher fluorescence intensity was formed during irradiation of Sudan I. If the dye would transform into species of different hydrophobicity or affinity to the shell material, there is a risk it could distort the results of stimuli response studies.

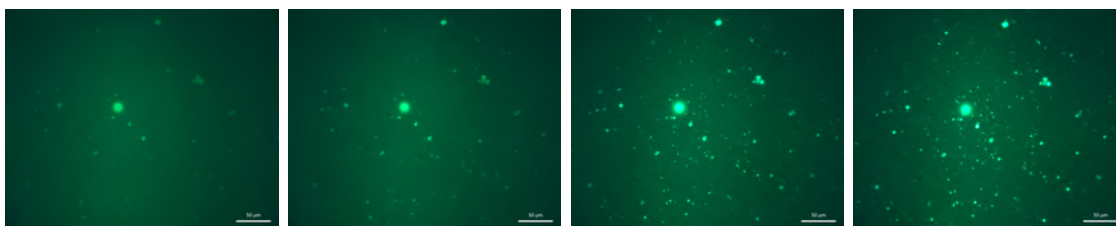


**Figure 4.17:** Increase of fluorescence intensity of PS microcapsules with Sudan I before UV (left) and consecutively: after 10 min, 30 min and 60 min of UV irradiation.

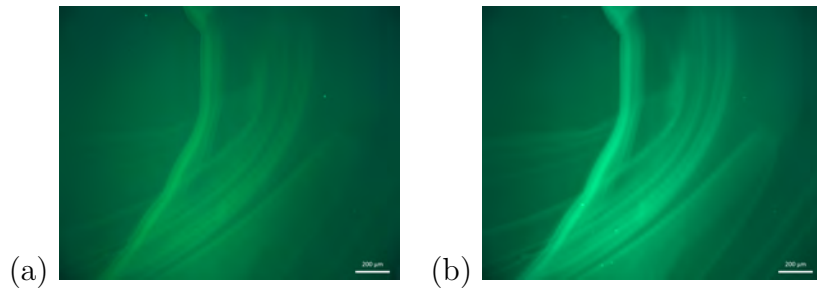


**Figure 4.18:** Sudan I dissolved in HD before (a) and after (b) 1.5h of UV irradiation.

#### 4.5.2 PMMA microcapsules

No significant differences in appearance of the bright field images of PMMA capsules were observed after 5h of UV irradiation. In some cases, subtle changes in shell surface could be observed as presented on Figure 4.19. Possibly, the molecular weight was not reduced enough and entangled chains were still holding the film together.

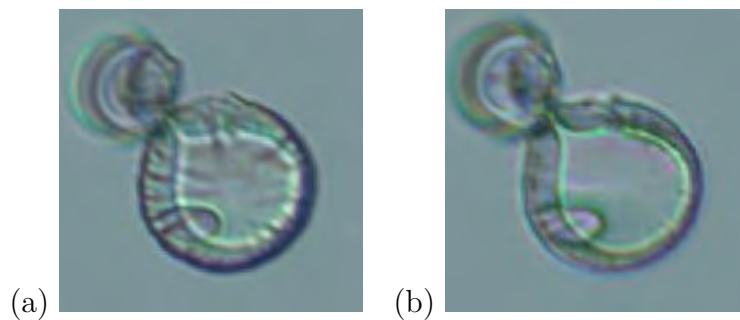


**Figure 4.19:** Bright field image of PMMA microcapsules (diameter 10 μm) before (a) and after (b) 5h of UV irradiation.

The fluorescence images were difficult to interpret, because of the Sudan I reaction to UV and the different exposure times used for acquisition. No dye outside the capsules was observed for PVA stabilized particles (Figure 4.20).

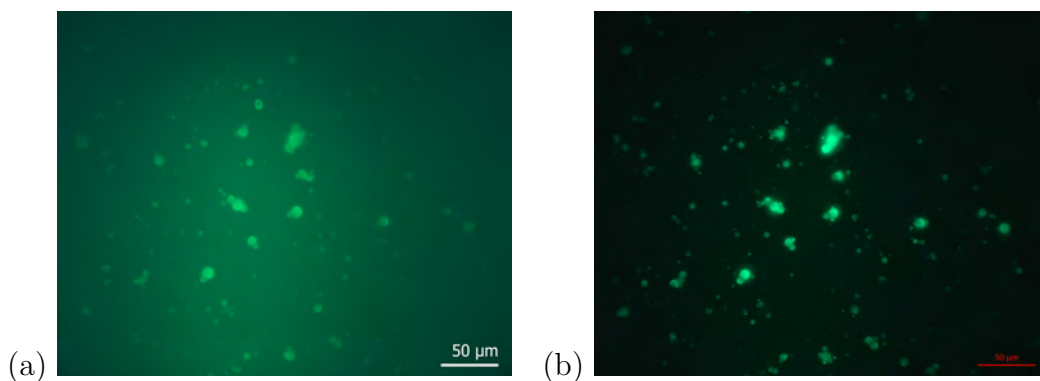


**Figure 4.20:** PMMA microcapsules stabilized with PVA, before (a) and after (b) 5h of UV irradiation.

In case of PMAA stabilized particles, patterns resembling oil leaks were observed after UV treatment (Figures 4.21), but this could be because of presence of the dye in the aqueous phase (Subsection 4.1.3). It is possible that the dye became visible after UV irradiation because of increase in fluorescence intensity discussed in Subsection 4.5.1. On the other hand, after magnification and processing of the images ((Figures 4.21 c, d)), it appears that the regions inside some of the capsules are darker after UV treatment. As seen on Figure 4.21b, the oil-leak patterns are not distributed evenly. Here the spot chosen for imaging with 50x, had no dye visible outside (Figure 4.21e, f), however fluorescence inside some of the capsules became apparently weaker. To be sure that release of the content occurred, the experiment should be repeated with another (or without) a dye, to exclude the possibility that lower fluorescence intensity of capsule interiors is related with Sudan I transformation into species with higher tendency to migrate towards the shell.

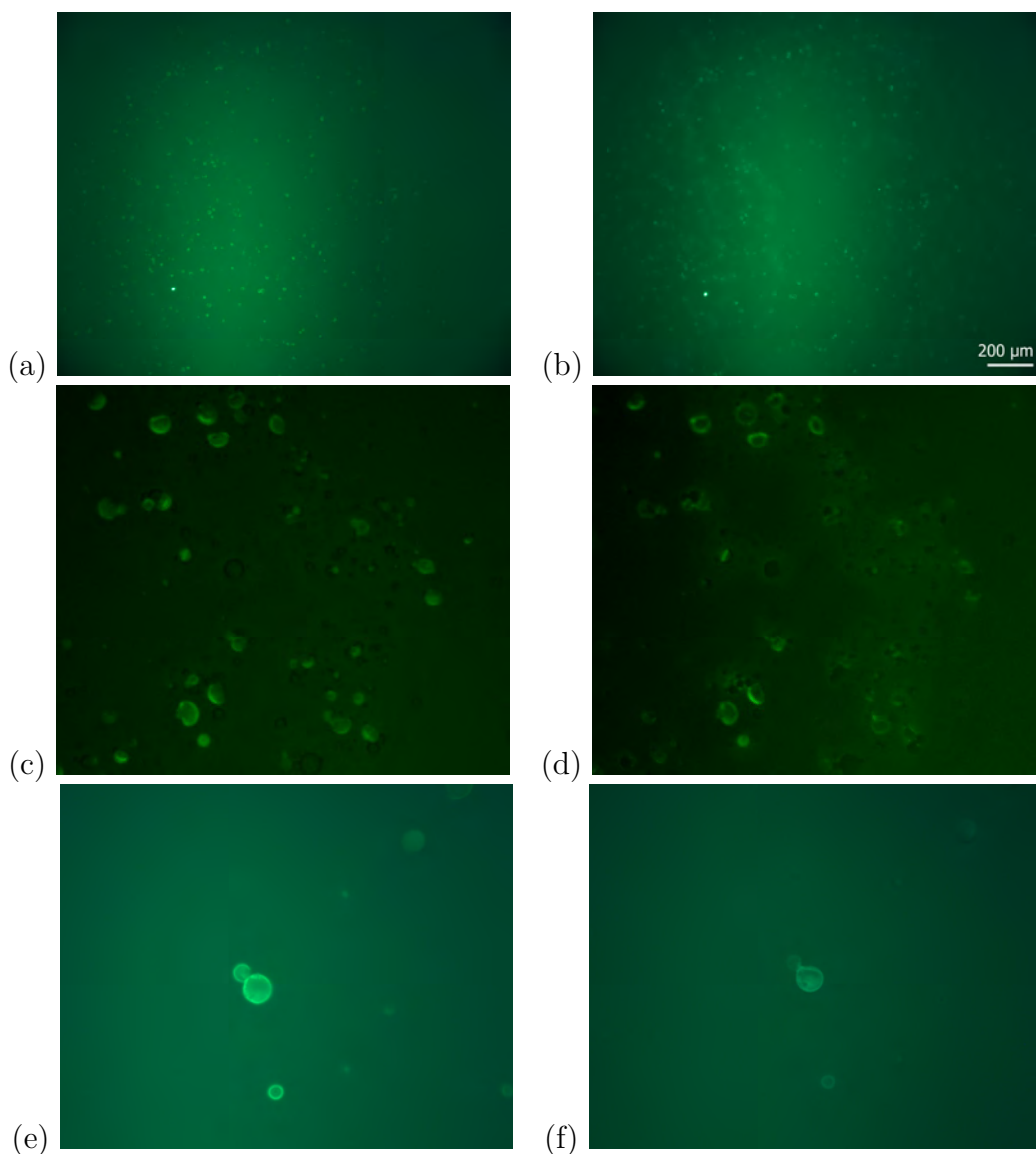


**Figure 4.21:** PMMA microcapsules stabilized with PMAA, before (a, c, e) and after (b, d, f) 5h of UV irradiation (particle diameters: 5-10 μm).

### 4.5.3 PS microcapsules

Bright field images of thin shell PS microcapsules did not change significantly after 4h of irradiation. Perhaps the dye hindered radical reactions in photooxidation. For some capsules a change in appearance of the wall region was observed (Figure 4.22). It could be a collapse of the upper region of the capsule shell, however it is difficult to interpret what happened while observing them at this angle.

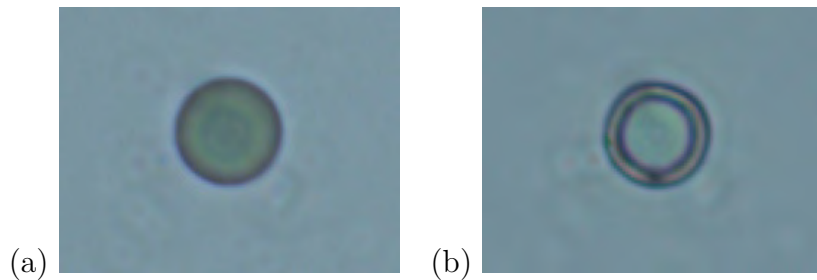


**Figure 4.22:** Bright field image of a PS microcapsule (diameter 10  $\mu\text{m}$ ) before (a) and after (b) 4h of UV irradiation.

No oil leaks were observed in fluorescence mode (the stabilizer was PVA). But it seems that the increase in fluorescence intensity after UV was greater than in case of PMMA (Figures 4.23), to the point that some areas are oversaturated and particle structures are not visible. The images obtained with a filter and in bright field did not reveal any other changes than these presented on Figure 4.22.

Considering that mechanical crushing of microcapsules from this batch resulted in increase of fluorescence as well (as mentioned in Section 4.4), it is possible that the enhanced brightness after UV arises from combination of shell degradation effect with typical increase in signal intensity from Sudan I after UV. Before irradiation it was problematic to find a spot where dry PS microcapsules would have fluorescent interior (however they were finally found), what is consistent with observations of the boundary of crushed capsule region presented in Section 4.4.

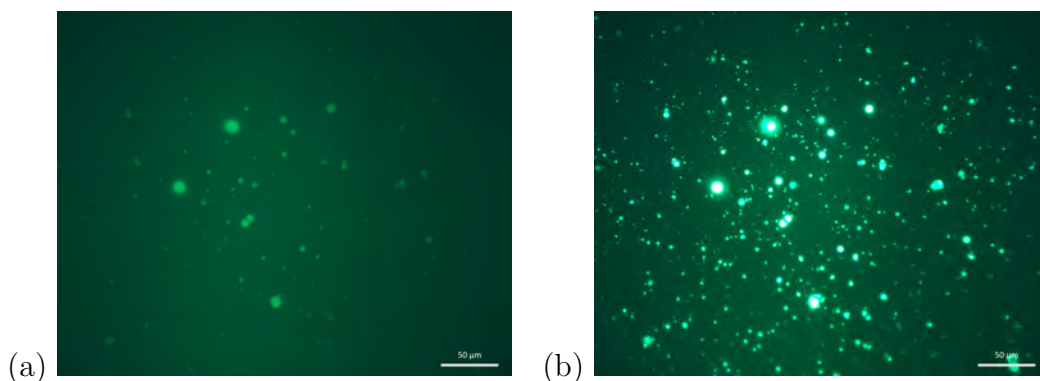


**Figure 4.23:** Thin-shell PS microcapsules before (a) and after (b) 4h of UV irradiation.

#### 4.5.4 PPHA microcapsules

Reaction of PPHA microcapsules with lycopene and without the dye was checked for various irradiation times (up to 10h), but no signs of released core were observed in any case. To exclude the possibility that irradiation time was too long [7], the capsules were irradiated for 3 and 10 min and left for few hours in darkness, but no degradation was observed after that. This was surprising considering that short irradiation times of PPHA films turned them into liquid of honey-like consistency [7]. Enhanced shell stability in comparison to polymer films have been also reported by Esser-Kahn *et al.* [66], who prepared microcapsules from self-immolative polymer reacting to chemical stimuli. The effect of microcapsule components and presence of other reactions apart from depolymerization would have to be further investigated.

After approximately 30 min of irradiation, a difference could be observed in increase of fluorescence intensity (similarly to Sudan I, no subsequent decrease was observed) and in change of appearance of the wall region, like in case of PS. Typical response of the capsules to UV is presented on Figure 4.24. The image is an overlay of fluorescence and bright field acquisition modes. It is unlikely that lack of apparent released oil is an imaging issue. It could be that even though shells are damaged, the oil stays inside because of interfacial tension. Perhaps leaks could be observed if more hydrophobic substrate was used, like polydimethylsiloxane (PDMS) thin film.

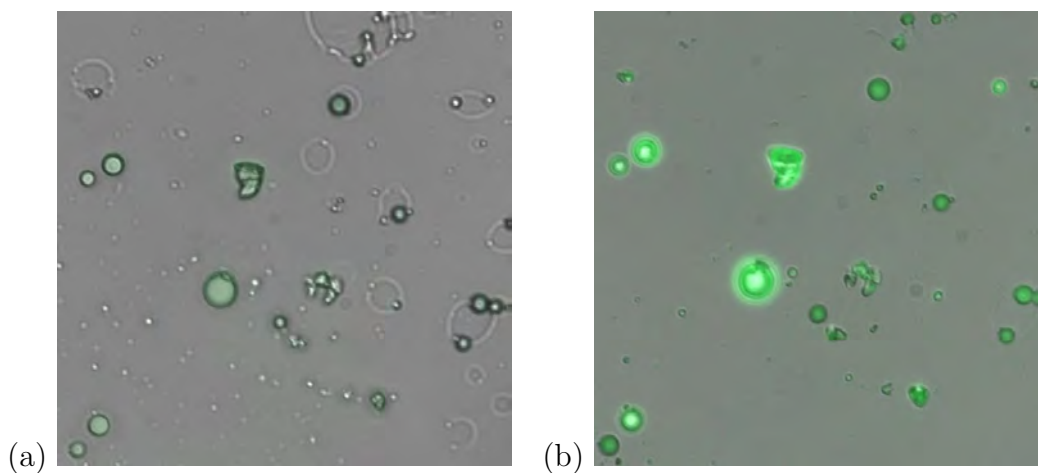


**Figure 4.24:** PPHA microcapsules without dye before (a) and after (b) 1.5h of UV irradiation.



# 5

## Conclusion

The purpose of this Master thesis project was to develop an experimental methodology to prepare microcapsules with shell material of UV-responsive polymers, to investigate their response to UV-irradiation, and to study the UV-triggered release. Previous work in the research group has focused on the release into a continuous liquid release medium. This project differed from those studies as the discharge of the cargo here was supposed to occur from dry microcapsules on a solid substrate. In this work, attention has been given to identify factors that should be taken into consideration while preparing microcapsules suitable for microscopic examination in dry state. A procedure to perform encapsulation using small quantities of polymers has been developed, and formulations for production of capsules with thinner shells and with low ceiling temperature have been found. Reproducible UV-irradiation experiments have been evaluated. A simple method to obtain a monolayer of dry microcapsules has been suggested and a strategy for visualization of the release using optical microscopy has been mapped out.

The main findings in formulation part are those related with microscopic visibility of core dyes substances, small-volume production, reduction of shell thickness, and production of microcapsules from polyphthalaldehyde (PPHA). It turned out that it is difficult to find a suitable dye that is sufficiently hydrophobic enough to remain in the alkane core and generate high fluorescence intensity. Sudan I appears to be a good candidate, but its unmapped reactivity towards UV-irradiation seems to interfere. Disperse Red 13 shows tendency to migrate towards the shell, while  $\beta$ -carotene and lycopene both have poor solubility in alkanes. The production in a small-volume setup required special measures when it comes to keeping the material amounts accurate, avoiding contamination and achieving good mixing. Shell thickness of polystyrene microcapsules could be reduced by weighting 2.55 less polymer than in the standard recipe. Formulation of PPHA microcapsules required higher concentration of polymer, otherwise acorn particles were formed, regardless of whether fast or slow evaporation of the solvent was performed. Because PPHA is fluorescent, its core-shell structure could be analyzed under optical microscope.

Regarding the release studies, it has been shown that a simple act of dropping a diluted microcapsule suspension on a tilted glass slide is enough to create a dry monolayer for microscopic studies of irradiation effects. Mechanical crushing with a glass rod or swelling the polymer with methanol are both suitable confirmatory methods to analyze the visual effect of release, but oil leakage can only be observed in the former one. Moreover, it has been proven that one can keep track of the

unique process of the same single microcapsule before and after UV-irradiation, so that conclusions can be drawn from very subtle changes in its appearance. The importance of choosing the appropriate technique of capturing microscopic images in this type of research has also been demonstrated. Release of dyed oil can be even unnoticed if wrong exposure time is used or no changes in histogram thresholds is done after acquisition of the image. This could be the case in some of the experiments with UV irradiation here. The capsules seemed to be not affected much by the UV light. Even though differences between some images captured before and after irradiation suggest that a release could occur, it is not certain that it actually happened. To be sure, the irradiation experiments would have to be performed again.

In the future work other dyes can be investigated. One could also focus on finding appropriate acquisition settings and postprocessing options to enhance the fluorescence signal from  $\beta$ -carotene, but awareness of its antiradical properties is important. If there would be a problem with fluorescence of the polymer overshadowing fluorescence of the dyed core, finding appropriate Filter Set could solve the issue. Nevertheless, oil released from bigger capsules should be visible in bright field mode without any dye. Regarding shell material, it would be of interest to formulate microcapsules from other polymers that showed promising results in the parallel project, especially from low molecular weight poly(methyl methacrylate) and photocrosslinkable poly(vinyl cinnamate) [7]. Further research might also explore why PPHA capsules exhibited only slight signs of degradation. In addition, it could be worth checking if the leakage of oil is easier to achieve using a more hydrophobic substrate.

The research provides a framework for future work on the UV-responsive microcapsules. The findings should be useful for any occasion when a small volume of microcapsule suspension must be prepared or when release from capsules laying on a solid substrate is to be investigated using optical microscopy. In the field of encapsulation, it is also an important finding that the standard internal phase separation by solvent (slow) evaporation method can be used to prepare microcapsules with shells from linear PPHA.

# Bibliography

- [1] A. P. Esser-Kahn, S. A. Odom, N. R. Sottos, S. R. White, and J. S. Moore, “Triggered release from polymer capsules”, *Macromolecules*, vol. 44, no. 14, pp. 5539–5553, 2011.
- [2] X. Yuan, K. Fischer, and W. Schärrtl, “Photocleavable microcapsules built from photoreactive nanospheres”, *Langmuir*, vol. 21, no. 20, pp. 9374–9380, 2005.
- [3] K. Katagiri, A. Matsuda, and F. Caruso, “Effect of uv- irradiation on polyelectrolyte multilayered films and hollow capsules prepared by layer-by-layer assembly”, *Macromolecules*, vol. 39, no. 23, pp. 8067–8074, 2006.
- [4] H. Kitano, T. Oehmichen, and N. Ise, “Photo-degradable polymer microcapsules”, *Macromolecular Chemistry and Physics*, vol. 192, no. 5, pp. 1107–1114, 1991.
- [5] Q. Yi and G. B. Sukhorukov, “Uv light stimulated encapsulation and release by polyelectrolyte microcapsules”, *Advances in colloid and interface science*, vol. 207, pp. 280–289, 2014.
- [6] S. J. Pastine, D. Okawa, A. Zettl, and J. M. Fréchet, “Chemicals on demand with phototriggerable microcapsules”, *Journal of the American Chemical Society*, vol. 131, no. 38, pp. 13 586–13 587, 2009.
- [7] S. Vavra, “Characterization of photodegradable polymers for uv-triggered release from microcapsules”, master thesis, Chalmers University of Technology, 2017.
- [8] A. Kamyshny and S. Magdassi, “Microencapsulation”, in *Encyclopedia of surface and colloid science*, P. Somasundaran, Ed., CRC press, 2015, 4636–4648.
- [9] M. A. Trojer, L. Nordstierna, M. Nordin, M. Nydén, and K. Holmberg, “Encapsulation of actives for sustained release”, *Physical Chemistry Chemical Physics*, vol. 15, no. 41, pp. 17 727–17 741, 2013.
- [10] B. Vincent, “Microgels and core-shell particles”, in *Surface Chemistry in Biomedical and Environmental Science*, J. P. Blitz and V. M. Gun’ko, Eds., Springer, 2006, pp. 15–18.
- [11] H. N. Yow and A. F. Routh, “Formation of liquid core–polymer shell microcapsules”, *Soft Matter*, vol. 2, no. 11, pp. 940–949, 2006.
- [12] A. Loxley and B. Vincent, “Preparation of poly (methylmethacrylate) microcapsules with liquid cores”, *Journal of colloid and interface science*, vol. 208, no. 1, pp. 49–62, 1998.
- [13] W. J. Duncanson, T. Lin, A. R. Abate, S. Seiffert, R. K. Shah, and D. A. Weitz, “Microfluidic synthesis of advanced microparticles for encapsulation and controlled release”, *Lab on a Chip*, vol. 12, no. 12, pp. 2135–2145, 2012.

- [14] A. Shulkin and H. D. Stöver, “Photostimulated phase separation encapsulation”, *Macromolecules*, vol. 36, no. 26, pp. 9836–9839, 2003.
- [15] N Zydowicz and E Nzimba-Ganyanad, “Pmma microcapsules containing water-soluble dyes obtained by double emulsion/solvent evaporation technique”, *Polymer Bulletin*, vol. 47, no. 5, pp. 457–463, 2002.
- [16] C. Perignon, G. Ongmayeb, R. Neufeld, Y. Frere, and D. Poncelet, “Microencapsulation by interfacial polymerisation: Membrane formation and structure”, *Journal of microencapsulation*, vol. 32, no. 1, pp. 1–15, 2015.
- [17] A. Dinsmore, M. F. Hsu, M. Nikolaidis, M. Marquez, A. Bausch, and D. Weitz, “Colloidosomes: Selectively permeable capsules composed of colloidal particles”, *Science*, vol. 298, no. 5595, pp. 1006–1009, 2002.
- [18] M. A. Trojer, Y. Li, C. Abrahamsson, A. Mohamed, J. Eastoe, K. Holmberg, and M. Nydén, “Charged microcapsules for controlled release of hydrophobic actives. part i: Encapsulation methodology and interfacial properties”, *Soft Matter*, vol. 9, no. 5, pp. 1468–1477, 2013.
- [19] P. J. Dowding, R. Atkin, B. Vincent, and P. Bouillot, “Oil core- polymer shell microcapsules prepared by internal phase separation from emulsion droplets. i. characterization and release rates for microcapsules with polystyrene shells”, *Langmuir*, vol. 20, no. 26, pp. 11 374–11 379, 2004.
- [20] A Goebel and K. Lunkenheimer, “Interfacial tension of the water/n-alkane interface”, *Langmuir*, vol. 13, no. 2, pp. 369–372, 1997.
- [21] R. Arshady, “Microspheres and microcapsules, a survey of manufacturing techniques: Part iii: Solvent evaporation”, *Polymer Engineering & Science*, vol. 30, no. 15, pp. 915–924, 1990.
- [22] B. Kronberg, K. Holmberg, and B. Lindman, *Surface chemistry of surfactants and polymers*. John Wiley & Sons, 2014, ch. 18.
- [23] L. K. Wang, Y.-T. Hung, and N. K. Shamma, *Physicochemical treatment processes*. Springer, 2005, vol. 3, p. 110.
- [24] J. Adair, E. Suvaci, and J. Sindel, “Surface and colloid chemistry”, in *The Encyclopedia of Materials: Science and Technology*, K. H. J. Buschow, R. Cahn, M. C. Flemings, B. Ilshner, S. Mahajan, P. Veyssiere, E. J. Kramer, and Knovel, Eds., Pergamon, 2001.
- [25] D. Shaw, *Introduction to Colloid and Surface Chemistry*, 4th. Saint Louis;San Diego; Butterworth-Heinemann, 2013, ch. 8.
- [26] S. U. Pickering, “Cxcvi. - emulsions”, *Journal of the Chemical Society, Transactions*, vol. 91, pp. 2001–2021, 1907.
- [27] F. Qi, J. Wu, G. Sun, F. Nan, T. Ngai, and G. Ma, “Systematic studies of pickering emulsions stabilized by uniform-sized plga particles: Preparation and stabilization mechanism”, *Journal of Materials Chemistry B*, vol. 2, no. 43, pp. 7605–7611, 2014.
- [28] E. Melzer, J. Kreuter, and R. Daniels, “Ethylcellulose: A new type of emulsion stabilizer”, *European journal of pharmaceuticals and biopharmaceutics*, vol. 56, no. 1, pp. 23–27, 2003.
- [29] R Pichot, F Spyropoulos, and I. Norton, “Competitive adsorption of surfactants and hydrophilic silica particles at the oil–water interface: Interfacial

- tension and contact angle studies”, *Journal of colloid and interface science*, vol. 377, no. 1, pp. 396–405, 2012.
- [30] A. Drelich, F. Gomez, D. Clause, and I. Pezron, “Evolution of water-in-oil emulsions stabilized with solid particles: Influence of added emulsifier”, *Colloids and Surfaces A: Physicochemical and Engineering Aspects*, vol. 365, no. 1, pp. 171–177, 2010.
- [31] B. Binks and S. Lumsdon, “Influence of particle wettability on the type and stability of surfactant-free emulsions”, *Langmuir*, vol. 16, no. 23, pp. 8622–8631, 2000.
- [32] B. P. Binks, “Particles as surfactants—similarities and differences”, *Current opinion in colloid & interface science*, vol. 7, no. 1, pp. 21–41, 2002.
- [33] A. N. Zelikin, J. F. Quinn, and F. Caruso, “Disulfide cross-linked polymer capsules: En route to biodeconstructible systems”, *Biomacromolecules*, vol. 7, no. 1, pp. 27–30, 2006.
- [34] K. E. Broaders, S. J. Pastine, S. Grandhe, and J. M. Fréchet, “Acid-degradable solid-walled microcapsules for ph-responsive burst-release drug delivery”, *Chemical Communications*, vol. 47, no. 2, pp. 665–667, 2011.
- [35] B. G. De Geest, W. Van Camp, F. E. Du Prez, S. C. De Smedt, J. Demeester, and W. E. Hennink, “Degradable multilayer films and hollow capsules via a ‘click’ strategy”, *Macromolecular rapid communications*, vol. 29, no. 12-13, pp. 1111–1118, 2008.
- [36] X. Tao, J. Li, and H. Möhwald, “Self-assembly, optical behavior, and permeability of a novel capsule based on an azo dye and polyelectrolytes”, *Chemistry-A European Journal*, vol. 10, no. 14, pp. 3397–3403, 2004.
- [37] M. F. Bédard, B. G. De Geest, A. G. Skirtach, H. Möhwald, and G. B. Sukhorukov, “Polymeric microcapsules with light responsive properties for encapsulation and release”, *Advances in colloid and interface science*, vol. 158, no. 1, pp. 2–14, 2010.
- [38] N. Fomina, C. McFearin, M. Sermsakdi, O. Edigin, and A. Almutairi, “Uv and near-ir triggered release from polymeric nanoparticles”, *Journal of the American Chemical Society*, vol. 132, no. 28, pp. 9540–9542, 2010.
- [39] K. Chen and S. Zhou, “Fabrication of ultraviolet-responsive microcapsules via pickering emulsion polymerization using modified nano-silica/nano-titania as pickering agents”, *RSC Advances*, vol. 5, no. 18, pp. 13 850–13 856, 2015.
- [40] C. Wochnowski, M. S. Eldin, and S. Metev, “Uv-laser-assisted degradation of poly (methyl methacrylate)”, *Polymer degradation and stability*, vol. 89, no. 2, pp. 252–264, 2005.
- [41] J. F. Rabek, *Polymer photodegradation: mechanisms and experimental methods*. Springer Science & Business Media, 2012, p. 144.
- [42] J. F. RABEK, *Photostabilization of Polymers: Principles and Application*. Springer Science & Business Media, 2012, ch. 1.
- [43] E. Yousif and R. Haddad, “Photodegradation and photostabilization of polymers, especially polystyrene”, *SpringerPlus*, vol. 2, no. 1, p. 398, 2013.
- [44] A. Torikai, M. Ohno, and K. Fueki, “Photodegradation of poly (methyl methacrylate) by monochromatic light: Quantum yield, effect of wavelengths, and light

- intensity”, *Journal of Applied Polymer Science*, vol. 41, no. 5-6, pp. 1023–1032, 1990.
- [45] C. E. Carraher Jr, *Introduction to polymer chemistry*. CRC press, 2012, ch. 7.
- [46] J. A. Kaitz, O. P. Lee, and J. S. Moore, “Depolymerizable polymers: Preparation, applications, and future outlook”, *MRS Communications*, vol. 5, no. 2, pp. 191–204, 2015.
- [47] Y. Zhang, L. Ma, X. Deng, and J. Cheng, “Trigger-responsive chain-shattering polymers”, *Polymer Chemistry*, vol. 4, no. 2, pp. 224–228, 2013.
- [48] A. M. DiLauro, J. S. Robbins, and S. T. Phillips, “Reproducible and scalable synthesis of end-cap-functionalized depolymerizable poly (phthalaldehydes)”, *Macromolecules*, vol. 46, no. 8, pp. 2963–2968, 2013.
- [49] C. E. Diesendruck, G. I. Peterson, H. J. Kulik, J. A. Kaitz, B. D. Mar, P. A. May, S. R. White, T. J. Martínez, A. J. Boydston, and J. S. Moore, “Mechanically triggered heterolytic unzipping of a low-ceiling-temperature polymer”, *Nature chemistry*, vol. 6, no. 7, pp. 623–628, 2014.
- [50] M. Tsuda, M. Hata, R. Nishida, and S. Oikawa, “Acid-catalyzed degradation mechanism of poly (phthalaldehyde): Unzipping reaction of chemical amplification resist”, *Journal of Polymer Science Part A: Polymer Chemistry*, vol. 35, no. 1, pp. 77–89, 1997.
- [51] W. Seo and S. T. Phillips, “Patterned plastics that change physical structure in response to applied chemical signals”, *Journal of the American Chemical Society*, vol. 132, no. 27, pp. 9234–9235, 2010.
- [52] R. Rottenfusser. (2017). Illumination and the microscope optical train; enhancing contrast, [Online]. Available: <http://zeiss-campus.magnet.fsu.edu/articles/basics/>.
- [53] M. Davidson. (2017). Mercury arc lamps, [Online]. Available: <http://zeiss-campus.magnet.fsu.edu/articles/lightsources/mercuryarc.html>.
- [54] J. R. Lakowicz, *Principles of fluorescence spectroscopy*. Springer Science & Business Media, 1992, pp. 1–2.
- [55] B. J. Berne and R. Pecora, *Dynamic light scattering: with applications to chemistry, biology, and physics*. Courier Corporation, 2000, pp. 6–8.
- [56] P. Demina, D. Grigoriev, G. Kuz'micheva, and T. Bukreeva, “Preparation of pickering-emulsion-based capsules with shells composed of titanium dioxide nanoparticles and polyelectrolyte layers”, *Colloid Journal*, vol. 79, no. 2, pp. 198–203, 2017.
- [57] (2017). C9750 sigma -  $\beta$ -carotene, [Online]. Available: <http://www.sigmaaldrich.com/catalog/product/sigma/c9750?lang=en&region=SE>.
- [58] M. H. Abraham, M. Amin, and A. M. Zissimos, “The lipophilicity of sudan i and its tautomeric forms”, *Physical Chemistry Chemical Physics*, vol. 4, no. 23, pp. 5748–5752, 2002.
- [59] (2017). Lycopene, [Online]. Available: <https://en.wikipedia.org/wiki/Lycopene>.
- [60] R. Vélez, S. Maiam, and R. Canela i Garayoa, “Influence of sample processing on the analysis of carotenoids in maize”, *Molecules*, 2012, vol. 17, núm. 9, p. 11261–11262, 2012.

- 
- [61] A. Martinez, “Donator- acceptor map and work function for linear polyene-conjugated molecules. a density functional approximation study”, *The Journal of Physical Chemistry B*, vol. 113, no. 10, pp. 3212–3217, 2009.
- [62] Y. Zhang, Y. Chen, P. Westerhoff, K. Hristovski, and J. C. Crittenden, “Stability of commercial metal oxide nanoparticles in water”, *Water research*, vol. 42, no. 8, pp. 2204–2212, 2008.
- [63] S. Tang, M. Yourdkhani, C. M. Possanza Casey, N. R. Sottos, S. R. White, and J. S. Moore, “Low ceiling temperature polymer microcapsules with hydrophobic payloads via rapid emulsion-solvent evaporation”, *ACS Applied Materials & Interfaces*, 2017.
- [64] L. Brancalion, G. Lin, and N. Kollias, “The in vivo fluorescence of tryptophan moieties in human skin increases with uv exposure and is a marker for epidermal proliferation”, *Journal of investigative dermatology*, vol. 113, no. 6, pp. 977–982, 1999.
- [65] E Severin and B Ohnemus, “Uv dose-dependent increase in the hoechst fluorescence intensity of both normal and brdu-dna”, *Histochemistry and Cell Biology*, vol. 74, no. 2, pp. 279–291, 1982.
- [66] A. P. Esser-Kahn, N. R. Sottos, S. R. White, and J. S. Moore, “Programmable microcapsules from self-immolative polymers”, *Journal of the American Chemical Society*, vol. 132, no. 30, pp. 10 266–10 268, 2010.





# Appendix A: Formulation details

**Table .1:** Composition and parameters used to produce microcapsules

No	Materials (shell/core/dye)	$M_S/M_C$	Dispersant*	Rotation speed	Remarks
Large volume setup (200ml two-necked flask)					
1	PMMA/HD/DR13	0.66	PMAA	7500	Dye added until the oil phase had light red color; rotary evaporated
2	PMMA/HD/DR13	0.66	PVA	6000-6500	Dye added until the oil phase had light red color
3	PMMA/HD	0.66	PMAA	5500-7500	-
4	PMMA/HD	0.66	PVA	5000-5500	-
5	PMMA/HD/DR13	0.66	PVA	5000-5500	Dye added until the oil phase had dark wine color
6	PMMA/HD	0.66	PMAA	5500-7500	Different homog. times test
7	PMMA/HD/Sudan I	0.66	PVA	5000-7000	$C_{dye} = 3.3$ g/l
8	PMMA/HD/Sudan I	0.66	PMAA	5500-7500	$C_{dye} = 3.3$ g/l
Small volume setup (5 ml two-necked flask)					
9	PMMA/OMCTS	0.53	PVA	5000-8000	-
10	PMMA/HD/ $\beta$ -carotene	0.66	PMAA	5000-7500	$C_{dye} = 1$ g/l
11-14	PMMA/HD	0.66	PMAA	5000-8000	Optimization
15	PMMA/HD	0.66	PVA	5000-5500	-
16	PMMA/HD/Sudan I	0.66	PMAA	5000-11000	-
17	PS/HD	0.66	PMAA	5000-10000	2% PMAA used
18	PS/HD	0.66	PMAA	5000-10000	-
19	PS/HD	0.25	PVA	5000-6000	-
20	PPHA/HD	0.66	PVA	5000-6000	-
21	PPHA/HD	0.66	PVA	5000-6000	Rotary-evaporated
22	PPHA/HD	1	PVA	5000-6000	-
23	PPHA/HD/lycopene	1	PVA	5000-6000	-

\* 1 wt% solution in MiliQ if not stated otherwise;  $M_S$ ,  $M_C$  - mass of the shell or core material; DR13 - Disperse Red 13;  $C_{dye}$  - concentration of dye in HD

**Table .2:** Typical emulsion composition ( $M_S/M_C = 0.66$ ) for large- and small volume setup

Component	Quantity in large volume	Quantity in small volume
Oil phase		
DCM	53 ml	1.99 ml (2.57 g)
HD	5 ml	0.19 ml
acetone	5 ml	0.19 ml
shell polymer	2.55 g	0.096 g
Aqueous phase		
dispersant	2 g	0.075 g
MiliQ water	200 ml	7.5 ml